

EEG Foundation Models: A Critical Review of Current Progress and Future Directions

Gayal Kuruppu^{1,†,*}, Neeraj Wagh^{2,†}, and Yogatheesan Varatharajah^{1,2}

¹Department of Computer Science & Engineering, University of Minnesota Twin Cities, MN, USA

²Department of Bioengineering, University of Illinois at Urbana-Champaign, Urbana, IL, USA

[†]Equal contributions

^{*}Correspondence: kurup016@umn.edu

ABSTRACT

Patterns of electrical brain activity recorded via electroencephalography (EEG) offer immense value for scientific and clinical investigations. The inability of supervised EEG encoders to learn robust EEG patterns and their over-reliance on expensive signal annotations have sparked a transition towards general-purpose self-supervised EEG encoders, i.e., EEG foundation models (EEG-FMs), for robust and scalable EEG feature extraction. However, the real-world readiness of early EEG-FMs and the rubric for long-term research progress remain unclear. A systematic and comprehensive review of first-generation EEG-FMs is therefore necessary to understand the current state-of-the-art and identify key directions for future EEG-FMs. To that end, this study reviews 10 early EEG-FMs and presents a critical synthesis of their methodology, empirical findings, and outstanding research gaps. We find that most EEG-FMs adopt a sequence-based modeling scheme that relies on transformer-based backbones and the reconstruction of masked sequences for self-supervision. However, model evaluations remain heterogeneous and largely limited, making it challenging to assess their practical off-the-shelf utility. In addition to adopting standardized and realistic evaluations, future work should demonstrate more substantial scaling effects and make principled and trustworthy choices throughout the EEG representation learning pipeline. We believe that developing benchmarks, software tools, technical methodologies, and applications in collaboration with domain experts may further advance the translational utility and real-world adoption of EEG-FMs.

1 Introduction

Electroencephalography (EEG) is a versatile tool for recording the brain's electrical activity and offers immense value to neuroscientists, biomedical engineers, and clinicians¹. The interpretation of multi-channel EEG recordings has historically been performed by trained experts because of their rich information content in the spatial and temporal dimensions. Despite decades of research into quantitative EEG features derived based on domain expertise, expert visual interpretation remains the gold standard for clinical EEG evaluation even to this day². However, in the last decade, EEG research has seen significant advances in deep learning-based approaches for extracting application-specific features from raw EEG data (EEG-DL)^{3,4}. Although this line of research held significant potential to augment traditional visual EEG review, it met with limited success due to several reasons. Much of the EEG-DL research relied on supervised learning on a very narrow group of EEG tasks that resulted from laborious expert-driven annotation efforts⁵. These efforts were clearly unscalable to cover the wide range of EEG tasks that might be needed in clinical or scientific EEG review. Furthermore, such supervised EEG encoders were highly susceptible to overfitting erroneous and noisy instances in training data, causing concerns regarding robustness and transferability to other tasks and datasets. This lack of robustness was further exacerbated by the variability of EEGs across recording sites, acquisition systems, subjects, and sessions, which led to an overall lack of trust in supervised EEG encoders^{6,7}. These limitations emphasized a need for EEG-DL models that rely less on expert EEG labels and yield robust and trustworthy EEG-DL models with high translational value.

The emerging paradigm of foundation models (FMs)⁸, based on label-free self-supervised learning (SSL) and efficient transfer learning, is a promising solution for these data-related challenges. Similar to the mainstream vision^{9–11} and language^{12–14} FMs, EEG foundation models (EEG-FMs) are trained to identify salient EEG features

from raw unlabeled EEG recordings by using various SSL pretext tasks, such as masked reconstruction or masked prediction, via a process known as *pretraining*. EEG-FMs learn to represent EEG data as compressed embeddings in a latent space by leveraging the intrinsic properties found in the raw data. Pretrained EEG-FMs can then be adapted for various downstream applications using only very small amounts of labeled data, thereby alleviating the burden of expert EEG annotations – the main bottleneck in supervised EEG-DL research. As such, EEG-FMs hold promise as powerful, off-the-shelf feature extractors (or *encoders*) that can support scientific research, next-generation robust brain-computer interfaces, and augmented neurological decision support.

Several first-generation EEG-FMs have been proposed over the last few years^{15–24}, whose cumulative count is shown in Figure 1. Despite the growing interest, many questions remain unanswered regarding the design choices within EEG-FMs, the learned representations, the performance on various real-world applications, and the overall guarantees on robustness and trustworthiness. For example, the choice of EEG input representations, the architectural components, and the SSL pretext tasks can vary significantly between models, and the effects of those choices on the learned features are unclear. The complexity, quality, and flexibility of the representations learned by EEG-FMs and their relation to brain physiology have not been sufficiently studied. Furthermore, the performance and generalizability of these EEG-FMs beyond the common public datasets and benchmarks have not been adequately evaluated. These questions and concerns call for a comprehensive review of the first-generation EEG-FMs focusing on the various architectural choices, pretraining approaches, evaluations, and trustworthiness aspects, to identify the rubrics for meaningful long-term progress in EEG-FM research and advance their translational value.

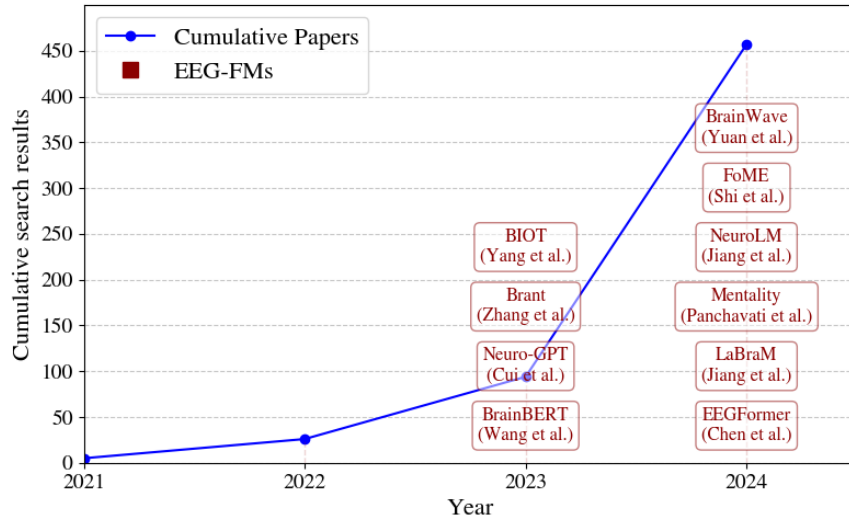


Figure 1. Cumulative EEG-FM search results from 2021 to September 30th, 2024. EEG-FMs are displayed chronologically in the plot based on their preprint publication dates.

To that end, this topical review focuses on the first generation of EEG-FMs and critically analyzes their building blocks, identifies key takeaways and research gaps, and suggests directions for future EEG-FM research. The contributions of this review are two-fold: a) it offers a principled understanding of EEG-FMs and the current state-of-the-art in a manner accessible to both EEG scientists and engineers, and b) it provides a domain-centric perspective and critique of existing work that can guide future generations of EEG-FMs. This review is organized as follows. Section 2 introduces the EEG recording procedures, the information content of EEGs, traditional quantitative EEG approaches based on feature engineering, the sources of data variability, and the different functional components of foundation models. Section 3 describes the search strategy we undertook to identify previously published EEG-FMs and provides brief summaries of those models. Section 4 provides a comprehensive analysis of each of the identified EEG-FMs along several dimensions, including training data, data preprocessing, input representations, model architectural components, and model evaluation strategies. Section 5 discusses the key takeaways and research gaps, and Section 6 lays out our view for future directions that would further advance the current state of the art.

2 Background

EEG is a common neurophysiological technique used to record electrical activity in the brain. It is widely used in clinical and research settings for diagnosing neurological disorders²⁵, studying brain function²⁶, and developing brain-computer interfaces²⁷. EEG measures voltage fluctuations resulting from ionic current flow within neurons²⁸ and is typically captured using electrodes placed directly on the scalp or intracranially. While intracranial EEG (iEEG) measures summated action potentials generated by small neuronal populations, scalp EEG measures the electrical activity generated by large neuronal populations that pass through multiple layers of the brain and head (i.e., cerebrospinal fluid, meninges, skull, scalp). The conduction of neuronal activity through these layers causes significant attenuation and spatial mixing of the EEG signal²⁹. As a result, scalp EEG has considerably different spatial resolution, amplitude, frequency, and noise content compared to intracranial EEG³⁰.

2.1 Contents and Sources of Variability in EEG Data

The EEG signal is a noisy, high-dimensional, spatio-temporal measurement of brain electrical activity. Several factors influence the contents of EEG recordings, including physiological, pathological, and artifactual components.

Physiological elements: The physiological elements present in EEG can be described using the various oscillatory components (delta, theta, alpha, beta, and gamma bands)³¹. The general attentional state of the subject during the recording (awake, drowsy, asleep) influences the frequency characteristics of EEG³². In addition, EEG also shows changes related to natural aging³³ and other benign changes in brain structure and function.

Pathological elements: The primary diagnostic value of EEG is due to its ability to capture various pathological brain activity patterns. These electrographic patterns include seizures, interictal epileptiform discharges (e.g., spikes and sharp waves), triphasic waves, rhythmic discharges, lateralized periodic discharges, background slowing, and other diffuse or focal abnormal electroencephalogram patterns²⁵.

Artifactual elements: EEG artifacts can be introduced by biological phenomena (e.g., eye blinks, head movement, muscle activity, cardiac signals), recording conditions (e.g., signal discontinuities, transient filter effects), or external sources (e.g., electromagnetic interference)³⁴. Eye- and muscle-related activities are the primary sources of artifacts found in EEGs, which introduce slow, high-amplitude, and fast, low-amplitude artifactual changes, respectively. In addition to these artifacts, certain medications, such as anti-depressants and anti-seizure medications, affect the EEG as well. For example, benzodiazepines and barbiturates are known to cause changes to the EEG³⁵.

The various practices and configurations used in clinical EEG studies introduce variabilities across EEG datasets. First, the hardware used to record EEGs can have preset configurations for filtering, analog-to-digital quantization, amplification magnitude, and broadband noise levels³⁶. Second, the EEG examination protocol may differ between clinical sites: the recording length could be different; recordings can have variable amounts of wake/sleep segments and eyes open/closed segments; and they may include cognitive tests and activation procedures such as sleep deprivation, photic stimulation, or hyperventilation. In addition, the EEG layout (i.e., number of leads and their positions) and reference leads may vary among sites. Finally, anatomical³⁷, genetic³⁸, and biochemical³⁹ differences introduce inter-individual variability. These factors make data ingestion and standardization for group-level modeling non-trivial, especially in intracranial EEG datasets, where lead locations are subject-specific.

2.2 Feature Extraction from EEG Signals

Characteristics of clinical EEGs are assessed visually by experts trained to detect pathological events and adverse deviations from healthy brain activity⁴⁰. However, in non-clinical settings, the EEG is characterized by signal features derived computationally and analytically from the raw data. Quantitative EEG *features* serve as lower-dimensional proxies of the raw signal that quantify pertinent brain activity and provide objective EEG assessments for various applications. Classical EEG features are derived from signal processing, statistics, and information theory domains. Examples include relative band-limited power, power ratios, independent components, sample entropy, and kurtosis, among others⁴¹. In select instances, classical EEG features isolate and quantify meaningful characteristics of underlying brain physiology, such as neuronal oscillations and functional connectivity, and are therefore considered robust and interpretable. In supervised deep learning (DL) models, EEG features are learned directly from raw EEG data to increase performance for a particular task⁴². While EEG-DL models may push

the boundaries of task performance, their black-box nature makes it difficult, or at least non-trivial, to understand their meaning and relevance to brain physiology. Furthermore, EEG-DL features may overfit the noise in EEG signals, making them less likely to generalize out of the box. Hence, the robustness, reliability, and interpretability of EEG-DL feature extractors remain open research problems.

2.3 Pillars of Foundation Modeling

In this section, we deconstruct the FM monolith into a set of universal, domain-agnostic building blocks/pillars. This set is minimally required for the systematic comparison of diverse existing EEG-FMs and to build new ones.

Representation of input data: EEG signals are acquired as a spatio-temporal data stream. Visual review of clinical EEGs is conducted primarily in this 'native' view. However, computational interpretation/analysis of EEGs can benefit from alternative, perhaps more informative, representations of raw data. For example, representing EEGs as a temporal stream of short spatio-spectral data segments (10s each) could make it easier for EEG-FMs to learn latent frequency patterns. Alternatively, representing EEGs using spatial covariance matrices can make it easier to extract latent connectivity patterns. Broadly, the choice/format of data representation at the input stage may greatly influence the quality and semantics of learned latent representations⁴³. In biosignal domains where data are sampled from underlying physiological processes, constructing informative input data views may itself require significant offline transformations or even domain-specific modeling, such as inverse or source modeling⁴⁴. Without these offline efforts, data-driven learning of latent representations via FMs may be inefficient or suboptimal.

Architectural and functional design of FMs: At an architectural level, FMs are typically built from several non-linear transformer blocks that can be readily stacked to scale the model depth and size. Transformer blocks themselves contain multiple feed-forward layers followed by a multi-head attention module⁴⁵. Vision FMs may use convolutional blocks to exploit the desirable spatial inductive bias of convolutions⁴⁶. Regardless of model size and any low-level architectural choices made, encoder-only FMs are understood to have only two high-level functional components: a backbone network and a final single fully connected layer. The backbone network serves as a feature extractor, providing low-dimensional embeddings (or representations) of the input data. The final layer, referred to as a *task head*, then uses these embeddings for task-specific purposes such as classification or regression.

Self-supervised learning (SSL): In the SSL paradigm, the supervision for training is strategically derived from the unlabeled input data (pseudo-labels) rather than from human-curated labels as is done in supervised learning⁴⁷. SSL objectives (pretext tasks) are commonly either contrastive or generative in nature. Contrastive pretext tasks use meaningfully augmented or noisy views of the input to learn robust data representations using encoder-only backbones⁴⁸. Generative pretext tasks mask various portions of the input and reconstruct/generate the masked portions using encoder and decoder-based backbones⁴⁹. In either case, SSL learns general intrinsic relationships within the data that help create a task-agnostic backbone network that serves as a general feature extractor. The structure of representations learned by SSL tasks and general principles for effective SSL task design are under active study. Regardless, the value of SSL is particularly high in the EEG domain as it improves model generalizability⁵⁰ and partially alleviates the need for expert EEG annotations that are expensive to obtain, subjective, and error-prone⁷.

Transfer learning and model adaptation: The backbone network, whether trained with or without self-supervision, allows for the re-use, transfer, and adaptation of EEG features (i.e., data-driven EEG knowledge) across semantically overlapping tasks⁵¹. The proportion of the backbone adapted for a specific application is flexible. For example, the backbone may be entirely fixed/frozen (*linear probing*), partially updated, or entirely updated (*fine-tuning*)⁵². This adaptation process may utilize slower learning rates or layer-specific learning rates to maximally preserve pretrained knowledge within the backbone. In either case, any pretext task-specific layers at the top are discarded and replaced with a new trainable linear head that performs classification or regression for the 'downstream' application. Using application-specific data splits and human-curated task-specific labels, the full model is then trained further until convergence. The development of algorithms for robust and efficient adaptation is an active area of research. Broadly, transfer learning and model adaptation techniques obviate the need to train new EEG-DL models from scratch by leveraging knowledge from pre-existing models.

Data and model scale: The scaling up of pretraining data and model size has contributed towards improved pretrained latent features, increased downstream task performance, sample efficiency, and model generalizability,

among other properties^{53–58}. Empirical scaling laws have established power-law relationships between FM error rates and three key modeling levers, namely the pretraining data size, model size, and compute^{55,59}, which suggest that an exponential increase in data and model size can indeed improve FM performance, albeit with diminishing returns. It is noteworthy that vision and language FMs are often multi-billion-parameter models and are pretrained on internet-scale datasets^{60–62}. Overall, the balance between data and model size to maximize performance under a fixed compute budget remains a critical consideration in FM research.

3 Review Approach & Summary of EEG-FMs

This section describes our search strategy and summarizes the EEG-FMs to date, highlighting the data used to train those models, model scale, architectural details, and evaluations.

3.1 Search Strategy

We conducted a comprehensive search across various web platforms, including Google Scholar, arXiv, DBLP, IEEE Xplore, bioRxiv, and medRxiv, to identify relevant research in journals, conferences, workshops, and preprints. We limited our search query to **EEG "Foundation Model"**. We then removed duplicate instances and manually reviewed the title, abstract, and introduction sections to confirm relevant EEG-FMs by identifying phrases similar to "*We developed an EEG foundation model...*" and "*The proposed approach forms the basis for an EEG foundation model...*". We note that our search starts from the year 2021 – the year the term *Foundation Model* was introduced⁸ – and includes studies that were published or archived on or before September 30th, 2024.

In addition to the set of foundation models identified above, we also included BrainBERT because of its common utilization as a baseline model in other EEG-FM evaluations^{17,19,23,24}. Furthermore, our review does not include foundation models developed on polysomnography (PSG) data^{63,64}, which are FMs designed specifically for sleep analysis. While it is possible to extract EEG representations from these FMs, they are not generalizable enough for broader EEG tasks since sleep EEG layouts do not cover the full extent of the head.

3.2 EEG-FM Summaries

Table 1 summarizes all ten EEG-FMs identified in our search. Although all the EEG-FMs share many commonalities, each FM is unique in its own right. In order to highlight the building blocks of each FM and their unique strengths, below we summarize each FM considering several factors, such as the amount of training data (in *channel-hours*, calculated as the total recording duration multiplied by the number of EEG channels; see supplement for details), model size (in terms of the number of trainable parameters), the types of EEG data (scalp EEG and/or iEEG), the way inputs are configured (raw time series, power spectra, or time-frequency representation), architectural components (convolutional and/or transformer blocks), the SSL tasks used for pretraining (masked reconstruction, auto-regressive modeling, and/or contrastive learning), and the evaluations performed.

BrainBERT¹⁵: As the first released EEG-FM, BrainBERT is relatively smaller than others, with 43.18M parameters and was trained using a modest dataset of 4.5k channel-hours of iEEG data. The inputs were represented as channel-wise spectrograms and a BERT⁶⁵-type model was trained to predict masked patches for different types of spectrograms such as Short-Time Fourier Transform⁶⁶ (STFT) and Superlets⁶⁷. The model comprised a transformer encoder with a shallow decoder with two linear layers. Evaluations showed generalizability to unseen subjects and unseen electrode locations; however, the test data were from the same distribution as the training data. The evaluations also showed that performing linear probing on BrainBERT embeddings was as good as training supervised deep neural networks (DNN) from scratch for most of the evaluation tasks, which are focused on predicting brain-evoked responses for watching movies. Additionally, their evaluations showed that fine-tuning BrainBERT embeddings can reach DNN performance from scratch with as little as 15% of the training data for one of the tasks. A task-agnostic intrinsic dimensionality⁶⁸ (ID)-based analysis showed that the BrainBERT embeddings of different brain regions had different IDs, compared to a relatively constant distribution across electrodes in randomly initialized weights.

Neuro-GPT¹⁶: This mid-size EEG-FM with 79.53M parameters was trained entirely using scalp EEG data from the full TUH corpus, including 541k channel-hours of clinical scalp EEG data. The model takes raw time series of the 22 EEG channels in the standard 10-20 layout as input and learns EEG representations using a combination

Table 1. Brief model summaries, including training data size, input configurations, data types, architectural components, and SSL tasks. Hyperlinks point to code and model weights, if available.

Model	Training Data (channel-hours)	Number of Parameters	Input Configuration	Data Type	Architectural Components	SSL Tasks
BrainBERT [link]	4.5k	43.18M	Single-channel spectrogram data	intracranial EEG	Transformer encoder and shallow decoder with two linear layers	Masked reconstruction
Neuro-GPT [link]	541k	79.53M	Fixed multi-channel time series data	Scalp EEG	Encoder with both convolution and transformer layers and GPT-2 as the decoder	Masked reconstruction (causally masked latent embeddings)
Brant [link]	281k	68M, 104M, 249M and 506M	Variable multi-channel time series data	intracranial EEG	Two transformer encoders for time and space and a linear decoder	Masked reconstruction
BIOT [link]	312k	3.3M	Variable multi-channel spectral data	Scalp EEG	Linear transformer, encoder-only architecture	Contrastive learning
EEGFormer	541k	N/A	Multi-channel spectral data	Scalp EEG	A transformer encoder and a shallow transformer decoder	Codebook-based reconstruction
LaBraM [link]	80k	5.8M, 46M and 369M	Fixed multi-channel time series data	Scalp EEG	Convolutional temporal encoder and transformer encoder layers and a linear decoder. A separate decoder for tokenization.	Masked reconstruction (token-level)
Mentality	N/A	N/A	Fixed multi-channel time series data	Scalp EEG	Convolutional layers and Mamba blocks in both encoder and decoder	Masked reconstruction
NeuroLM [link]	546k	250M, 500M and 1.7B	Variable multi-channel time series data	Scalp EEG	Vector quantization for tokenization with convolutional temporal encoder and transformer spatial encoder	Autoregressive reconstruction (token-level)
FoME	N/A	476M and 745M	Variable multi-channel time series data	Scalp EEG and intracranial EEG	Temporal and Spatial transformer encoder and a linear decoder	Masked signal reconstruction
BrainWave	878k	N/A	Variable multi-channel spectrogram data	Scalp EEG and intracranial EEG	Transformer encoder with channel attention and a lightweight decoder	Masked reconstruction (whole spectrogram)

of convolution and transformer layers. Those representations are then used as input to a GPT-2⁶⁹ decoder which autoregressively predict the masked latents. It is noteworthy that the decoder has more parameters than the encoder in this setup compared which is not a common practice in other EEG-FMs. This model was evaluated only on EEG data from a BCI motor imagery task with four classes with a different channel configuration than the training data. However, the downstream data were transformed to the original input configuration using an inverse-forward approach⁷⁰. The results showed that fine-tuning or linear probing the pretrained model performed better than models trained from scratch, including some EEG-specific fully-supervised DL approaches.

Brant¹⁷: Brant is a relatively larger FM with 500M parameters and was trained using 281k channel-hours of iEEG data. However, its pretraining data were limited to a single dataset comprising 9 subjects. This model also takes raw EEG time series as input and is able to take inputs with different channel configurations. The model consisted of a temporal encoder that learns long-term temporal dependencies, a spatial encoder that learns spatial correlations, and a simple linear decoder. The spatial encoder used in this model to capture spatial relationships is a novel contribution compared to previous EEG-FMs. This model also has three scaled-down versions with of 68M, 104M, and 249M parameters, respectively, that are trained on the same data. These models were evaluated on short/long term signal forecasting, frequency phase forecasting, imputation, and seizure detection tasks.

BIOT¹⁸: This is the smallest of the ten EEG-FMs considered in this review, with only 3.3M parameters, and was pretrained using a contrastive learning objective. The BIOT model introduced a novel approach to take input data with variable lengths and a variable number of channels; it tokenizes each channel into fixed-length segments representing frequency energy vectors, organizes them into “sentences”, and uses channel and position embeddings to preserve spatio-temporal information. This model also utilized linear transformers to reduce training time. The model was then evaluated on multiple clinical tasks, such as seizure detection and seizure type classification, in which the model showed superior performance even without pretraining, and showed even better performance with pretraining, compared to previous fully-supervised DL models.

EEGFormer¹⁹: This model was also pretrained on the whole TUH corpus, which includes approximately 541k channel-hours of clinical scalp EEG data. It included a transformer encoder and a shallow transformer decoder and it was pretrained using a masked-reconstruction objective. The encoder generated latents of input EEG patches are used to train a vector quantizer to match neural codes generated by a neural codebook. The decoder then reconstructs the original EEG patches using these neural codes. Evaluations included several downstream tasks derived from the TUH corpus and an out-of-distribution (OOD) evaluation on a neonatal seizure detection task. Additional experiments also included interpretability analyses using the learned codebook.

LaBraM²⁰: This model utilized the most diverse, yet a small dataset for pretraining, including 80k channel-hours of scalp EEG data – a subset of the TUH corpus. It was developed in three different scales, with 5.8M, 46M to 369M parameters, respectively. The model consisted of two parts, the neural tokenizer and the neural transformer (LaBraM pretraining model). Both took temporally and spatially patched raw time series data as input and then passed through convolutional temporal encoder of which the outputs are then concatenated with temporal and spatial embeddings and then passed through a set of transformer blocks. The neural tokenizer is trained to reconstruct the amplitude and phase of the patch through a separate decoder, during which the codebook is trained. The neural transformer is trained from scratch, and similar to the neural transformer, except to predict the neural codes inferred using the frozen neural tokenizer, by masked prediction. Although the evaluations demonstrated performance gains various subsets of the TUH corpus, it is unclear whether these results generalize to OOD data.

Mentality²¹: This model aims to capture the complex spatio-temporal dynamics of EEG signals using a Mamba⁷¹-based state-space model. The architecture of Mentality drew inspiration from other models such as SaShiMi⁷², U-Net⁷³, and EEGNet⁷⁴ with the inclusion of Mamba blocks. However, the model was trained and evaluated exclusively on the TUSZ dataset. Furthermore, the unavailability of code or pretrained models limits reproducibility and further evaluations, and makes it inaccessible for broader use as a foundation model.

NeuroLM²²: This model was inspired by a previous EEG-FM, LaBraM. However, NeuroLM was trained on 7x more data and is one of the largest EEG-FMs with 1.7B parameters, along with 250M and 500M parameter versions. NeuroLM utilized a text-aligned neural tokenizer, which is trained using temporal and frequency reconstruction along with a text/EEG domain classifier that is trained adversarially. The neural tokenizer is similar to that of LaBraM, except for the text alignment component and also included temporal reconstruction in addition to frequency reconstruction. However, despite this novel contribution, the evaluations indicated that the model loses some performance on downstream tasks compared to LaBraM and other state-of-the-art models.

FoME²³: This model included two versions with 476M and 745M parameters, respectively. The size of the training data was not provided in the manuscript. The model takes masked time series patches and their power spectral densities as input, which are transformed by a temporal encoder. The outputs of the temporal encoder are then reorganized by channels and given as inputs to a spatial encoder to reconstruct masked time patches. FoME was evaluated on multiple downstream tasks, including classification, forecasting, and imputation; however, the evaluations were performed on in-distribution data, limiting any broader conclusions.

BrainWave²⁴: This model was pretrained using a large dataset of size 878k channel-hours, including both scalp EEG and iEEG. It includes a transformer encoder and a channel attention module that transform EEG spectrograms into latent representations, which are then decoded by a lightweight decoder. This encoder-decoder architecture was trained using a masked-reconstruction objective. BrainWave is one of the few EEG-FMs trained and evaluated on both scalp EEG and iEEG signals, demonstrating the benefits of joint pretraining over unimodal approaches. The model has been extensively evaluated under different settings, such as cross-subject, cross-hospital, cross-subtype

and few-shot classification, showcasing the generalizability and robustness across various clinical tasks.

4 Comparative Analysis of EEG-FMs

This section surveys the EEG-FMs and compares their design and construction along three major axes covering the pillars of foundation modeling described in Section 2: a) preparation and representation of input data, b) model architecture and self-supervised pretraining, and c) model evaluations. The various considerations along these axes are illustrated in Figure 2. We then highlight the key takeaways from those comparisons.

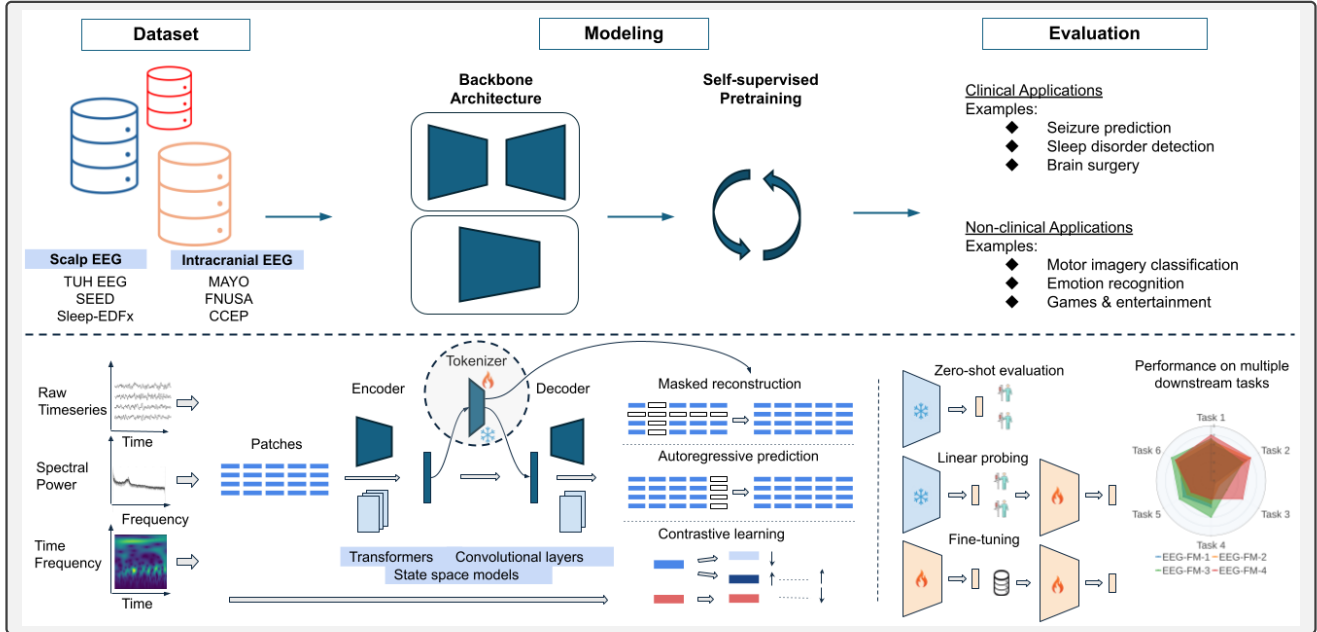


Figure 2. Overview of comparative analysis. We analyze EEG-FMs along three major axes; input data, modeling and evaluation. EEG data is represented in one of three forms: raw time series, the magnitude power spectrum, and time-frequency representation. The FM architecture may include convolutional blocks to learn low-level patterns and/or transformer blocks to learn higher-level relationships. The FMs are pretrained using SSL approaches; the common SSL approaches used are masked-reconstruction, auto-regressive modeling, and contrastive learning. The pretrained models are then evaluated on various downstream tasks, including clinical and non-clinical tasks. We compare and contrast all ten EEG-FMs along these factors and discuss their strengths and weaknesses.

4.1 Preparation and Representation of Input Data

Datasets: The data used for pretraining functions as the knowledge base of an FM, making it a highly crucial component in developing a foundation model. Key factors such as diversity, volume, relevance, and, most importantly, quality of the data significantly influence the generalizability of the patterns learned by an FM. Table 2 shows the datasets that were used in the pretraining and evaluation phases of the ten EEG-FMs reviewed in this article.

Most EEG-FMs (e.g., LaBraM, EEGFormer, Neuro-GPT, Mentality, BIOT, and NeuroLM) were trained only on scalp EEG data, although some (e.g., Brant and BrainBERT) were trained exclusively on iEEG data. Two EEG-FMs, FoME and BrainWave, were trained on both scalp and intracranial EEG data. A large portion of the training data in the models utilized scalp EEG was taken from the Temple University Hospital (TUH) EEG corpus⁵, which has a total of 541k channel-hours of scalp EEG data. Other scalp EEG datasets used for pretraining include CHB-MIT⁷⁵ and various small datasets collected for research purposes. Some FMs utilized EEG data available within PSG datasets such as SHHS⁷⁶, Sleep-EDF⁷⁷, and CAP Sleep⁷⁸. Additionally, public or private iEEG data accounted for large portions of training data in some models, such as Brant and BrainWave. The common publicly available iEEG datasets used for pretraining were MAYO⁷⁹, FNUSA⁷⁹, Brain TreeBank⁸⁰, and CCEP⁸¹. Training data volume

ranged from 14k channel-hours in BrainBERT to 878k channel-hours in BrainWave. BrainWave utilized the most diverse set of pretraining data, including clinical scalp EEG datasets, sleep EEG datasets, various smaller-scale scalp EEG repositories, and several iEEG datasets. LaBraM and NeuroLM also utilized moderately diverse datasets for pretraining, although all of the datasets were scalp EEG datasets.

Preprocessing and normalization: The content of EEG data is highly sensitive to the choice of pre-processing and normalization steps performed ahead of model training or evaluation. The choices made on resampling, bandpass and notch filtering, artifact removal, and data segmentation into patches or epochs, can directly impact the representations learned by an EEG-FM. Although some models did not comprehensively describe the preprocessing steps, most models applied standard procedures such as bandpass filtering (0.5Hz to a higher cutoff frequency), powerline interference removal via notch filters (50Hz or 60Hz, including harmonics), and downsampling to 200 Hz or 250 Hz to standardize sampling rates across datasets. EEG signals are then segmented into smaller epochs, typically between 1 and 10 seconds. However, none of the EEG-FMs performed explicit artifact removal or exclusion of outlier data, except in cases of expertly-labeled bad data or missing channels. Other less common preprocessing steps included DC offset removal and linear trend removal by FoME and Neuro-GPT. Data normalization practices after preprocessing were not described in several manuscripts. Neuro-GPT applied the commonly used z-transform along the time dimension to normalize the EEG signals, while NeuroLM, BIOT, and LaBraM applied scaling with a constant factor based on the range of input values.

Input representation: EEG is a spatio-temporal data modality, which can be denoted as $X \in \mathbb{R}^{C \times T}$ with C channels and T time points. In addition to the spatial and temporal information, spectral information is also useful in interpreting EEG data, which is used most often as expert-derived features in statistical ML models. Furthermore, time-frequency representations, such as spectrograms or wavelet⁸² transforms, are also used to preserve information on all three domains. All EEG-FMs used one or a combination of these representations as input.

The most widely used input representation is the multivariate time series data format, which was adopted by six out of the ten EEG-FMs. With the adoption of transformer architecture, the windows that are segmented from the original recording require further segmentation into smaller patches, also known as tokens. These patches or tokens can then be added with temporal and spatial information with positional embeddings, which allows the models to be trained using EEG data with different channel configurations. This approach was adopted by models such as Brant, NeuroLM, and FoME, which allowed training using datasets with a varying number of channels. Two models, BIOT and EEGFormer, utilized power-spectral data as input instead of the original time series patches, while two other models, Brant and FoME, added power-spectral data to complement the raw time series inputs. Some EEG-FMs, such as LaBraM, Neuro-GPT, and Mentality, standardized different EEG datasets with different channel configurations to a fixed set of input channels. Two other models, BrainBERT and BrainWave, utilized channel-wise time-frequency representations of 1-5 seconds of EEG data as input. Various experiments performed in BrainBERT evaluations utilized spectrograms generated using classical methods like STFT as well as scalograms⁸² generated using modern methods such as Superlets.

4.2 Modeling and Pretraining

Architectural components: The model architecture and training objectives play a central role in determining the effectiveness of a foundation model in extracting information from the input data⁸. EEG-FMs utilized various components at different stages of the pipeline, including tokenizers, local representation learning modules, spatial and/or temporal attention modules to learn dependencies, and task heads. Almost all the EEG-FMs we review in this article are transformer-based, except Mentality, which uses a combination of convolutional layers and a mamba-based architecture. In the transformer-based models, the input signal is divided into a fixed number of small patches/tokens to construct the input sequence. Some models that utilized raw time series inputs leveraged convolutional layers to learn morphological features (e.g., Neuro-GPT, LaBraM, Mentality, NeuroLM).

Neural tokenizers: Some models, such as LaBraM, NeuroLM, and EEGFormer, integrated separate tokenizers to transform the input signals into discrete tokens or codes. These EEG-FMs adapted a VQ-VAE¹²³-like architecture to train a neural tokenizer, which mapped input patches into a fixed set of discrete embeddings called the *codebook*. During tokenizer training, latent codes are mapped to nearest neighbor embeddings from the codebook to reconstruct

Table 2. Datasets used to train and evaluate EEG-FMs. We highlight datasets that are not publicly available in bold, clinical and non-clinical datasets in pink and blue backgrounds, respectively, and use superscripts * and # to denote evaluations in internal and external datasets, respectively.

Dataset/EEG-FM	BrainBERT	Neuro-GPT	Brant	BIOT	EEGFormer	LaBraM	Mentality	NeuroLM	FoME	BrainWave
Scalp EEG										
TUEG ⁸³		<i>train</i>			<i>train</i>			<i>train</i>	<i>train</i>	<i>train</i>
TUAB (Abnormal/normal classification - binary)				<i>eval[#]</i>	<i>eval[*]</i>	<i>eval[*]</i>		<i>eval[*]</i>		
TUAR (EEG artifact classification - multiclass)					<i>eval[*]</i>	<i>train</i>				
TUEP (Epilepsy classification - binary)						<i>train</i>				
TUEV (EEG Events classification - multiclass)				<i>eval[#]</i>		<i>eval[*]</i>		<i>eval[*]</i>	<i>eval[*]</i>	
TUSL (EEG slowing classification - multiclass)					<i>eval[*]</i>	<i>train</i>		<i>eval[*]</i>		
TUSZ (Seizure type classification - multiclass)					<i>eval[*]</i>	<i>train</i>	<i>train/eval[*]</i>			
CHB-MIT ⁷⁵ (Pediatric seizure detection - binary)				<i>eval[#]</i>				<i>train</i>		<i>eval[#]</i>
Sleep-EDFx ⁷⁷ (Sleep stage classification - multiclass)									<i>train/eval[*]</i>	<i>train</i>
Siena Scalp EEG ⁸⁴ (Seizure classification - binary)						<i>train</i>		<i>train</i>		<i>train</i>
SHHS ⁵⁷⁶ (Sleep stage classification - multiclass)				<i>train</i>						
PREST (Abnormal event detection - binary)				<i>train</i>						
CAP Sleep ⁷⁸ (Sleep stage classification - multiclass)										<i>train</i>
HMC ⁸⁶ (Sleep stage classification - multiclass)								<i>eval[#]</i>		<i>train</i>
SRM ⁸⁷ (Resting state EEG data)										<i>train</i>
Schizophrenia-81 (Schizophrenia classification - binary)										<i>train</i>
Stroke-50 ⁸⁸ (Hand movement classification - binary)										<i>train</i>
PD-31 ⁸⁹ (Parkinson disease classification - binary)										<i>train</i>
IowaDataset ⁹⁰ (Unknown task/s)										<i>train</i>
UNMNDdataset ⁹¹ (Parkinson disease classification - binary)										<i>train</i>
AD-184 ⁹² (Alzheimer's disease classification - binary)										<i>train</i>
Neonate dataset ⁹³ (Seizure detection - binary)					<i>eval[#]</i>					
IIIC Seizure ⁹⁴ (IIIC pattern classification) - multiclass				<i>eval[#]</i>						
Absence-16 (Seizure type classification - multiclass)										<i>eval[#]</i>
Clonic-6 (Seizure type classification - multiclass)										<i>eval[#]</i>
Atonic-5 (Seizure type classification - multiclass)										<i>eval[#]</i>
DRE-Clinical (Seizure detection and localization - binary)										<i>eval[#]</i>
SD-71 ⁹⁵ (Sleep deprivation detection - binary)										<i>eval[#]</i>
ADHD-Adult ⁹⁶ (ADHD classification - binary)										<i>eval[#]</i>
ADHD-Child ⁹⁷ (ADHD classification - binary)										<i>eval[#]</i>
Schizophrenia-29 ⁹⁸ (Schizophrenia classification - binary)										<i>eval[#]</i>
Depression-122 ⁹⁹ (Depression classification - binary)										<i>eval[#]</i>
MDD-64 ¹⁰⁰ (Major depression detection - binary)										<i>eval[#]</i>
AD-65 ¹⁰¹ (Alzheimer's disease classification - binary)										<i>eval[#]</i>
BCI Competition IV-1 ¹⁰² (Movement classification - binary)						<i>train</i>		<i>train</i>		
Emobrain ¹⁰³ (Emotion classification - multiclass)						<i>train</i>		<i>train</i>		
Grasp/Lift EEG Challenge ¹⁰⁴ (Grasp classification/regression)						<i>train</i>		<i>train</i>		
Inria BCI Challenge ¹⁰⁵ (Next letter classification - multiclass)						<i>train</i>		<i>train</i>		
EEG Motor Imagery Dataset ¹⁰⁶ (Classification - multiclass)						<i>train</i>		<i>train</i>		
Visual Categorization EEG Data ¹⁰⁷ (Classification - multiclass)						<i>train</i>		<i>train</i>		
Resting State EEG Data ¹⁰⁸ (Eye state classification - binary)						<i>train</i>		<i>train</i>		
SEED Series ¹⁰⁹⁻¹¹¹ (Emotion classification - multiclass)						<i>train/eval[*]</i>		<i>train/eval[*]</i>	<i>train/eval[*]</i>	
SPIS Resting State Dataset ¹¹² (CVS and HRT regression)						<i>train</i>		<i>train</i>		
Brain-Invaders ¹¹³ (Target vs. non-target classification - binary)						<i>train</i>		<i>train</i>		
Multiple data sources ¹¹⁴⁻¹¹⁸ (Unknown tasks)						<i>train</i>		<i>train</i>		
MoBI ¹¹⁹ (Gait angle regression)						<i>eval[#]</i>				
BCI Competition IV Dataset 2a ¹²⁰		<i>eval[#]</i>								
Workload ¹²¹ (Workload classification - binary)								<i>eval[#]</i>		
Intracranial EEG										
Brain TreeBank ⁸⁰ (EEG classification - multiclass)	<i>train/eval[*]</i>									
Private single dataset without source (Unknown)				<i>train/eval[*]</i>						
Private dataset collection without source (Unknown)										<i>train</i>
MAYO ¹²² (Seizure detection and multi-class classification)				<i>eval[#]</i>					<i>train/eval[*]</i>	<i>eval[#]</i>
FNUSA ¹²² (Seizure detection and multi-class classification)				<i>eval[#]</i>					<i>train/eval[*]</i>	<i>eval[#]</i>
CCEP ⁸¹ (Seizure onset zone localization - binary)										<i>train</i>

some known feature of the input, such as power amplitudes and phase in LaBraM and temporal and spectral reconstruction in NeuroLM. All of these models utilized neural codebooks in the context of reconstructing raw time series inputs using a transformer-like architecture. While NeuroLM and EEGFormer utilized codebook embeddings to map the encoder outputs to discrete codes prior to decoding, LaBraM utilized pretrained codebook embeddings of input signal patches as targets during model pretraining.

Spatial encoding: EEG-FMs implemented different spatial encoding strategies, although they differ in how explicitly they handle spatial information. Brant and FoME, for example, used transformer encoders with spatial attention but without dedicated spatial embeddings. In contrast, LaBraM, BIOT, and NeuroLM injected spatial information through explicit spatial embeddings to enhance positional encoding and capture the topographic layout of EEG channels. Among them, only BIOT supported multiple electrode configurations, while LaBraM and NeuroLM are limited to a fixed 10–20 montage format for spatial encoding. Models such as Neuro-GPT and Mentality learned spatial dependencies implicitly using convolutional layers, without dedicated spatial embeddings. BrainWave incorporated spatial attention mechanisms to model inter-channel dependencies directly. In contrast, BrainBERT and EEGFormer omit spatial modeling altogether, using only transformer layers without convolution or spatial priors.

Self-supervision: SSL approaches are the key components that enable the development of foundation models by learning common features represented in massive unlabeled datasets⁸. Most EEG-FMs (seven out of ten) employed reconstruction of masked data as the primary SSL approach. EEGFormer model was pretrained by minimizing the reconstruction loss between input signals and signals decoded from codebook mappings of transformer-encoded input patches. NeuroLM employed an autoregressive approach to predict future patches from past patches, including EEG-text an alignment objective, and BIOT adopted a contrastive learning approach where the embeddings of masked inputs and the same inputs with different augmentations are minimized (i.e., the SimCLR⁴⁸ pretraining approach). Only one model – Neuro-GPT, employed masked data reconstruction in the latent space. Additionally, the LaBraM model also employed a masked-signal reconstruction approach; however, the codebook embeddings of the masked input patches from a previously-trained neural tokenizer were used as reconstruction targets.

Masking: The granularity of the learned representations in the EEG-FMs is influenced by the type and extent of masking used during self-supervised pretraining¹²⁴. In models based on masked-signal reconstruction, masking is typically applied to random patches across temporal and spatial dimensions, as opposed to masking entire channels or full time segments. For example, Brant and FoME applied a ~40% uniform random masking, zeroing-out the masked input signal patches across time and channel dimensions. LaBraM similarly utilized a 50% patch-level masking, while BrainWave, despite operating in the spectrogram domain, performed masking entire spectrograms of several channels. On the other hand, BrainBERT applied a more fine-grained masking strategy, masking 5% from the time domain and 5% from the frequency domain, effectively masking ~10% of the input spectrogram. Mentality applied random channel masking, targeting specific channels rather than patches. NeuroLM introduced a stair-step masking scheme, in which next token is auto-regressively predicted in a channel-conditioned manner, whereas Neuro-GPT utilized a causal masking approach in the latent space, consistent with autoregressive generation.

Patching and context length: The temporal resolution of tokens or patches, i.e., how much EEG data each patch contains, varies between models, reflecting different design choices in model architecture and target tasks. Brant and FoME utilized patches corresponding to six seconds of EEG, while BrainBERT utilized 5-second STFT/Superlet windows. Models such as LaBraM, NeuroLM, BIOT, and BrainWave adopted a finer resolution, using 1-second segments per patch, whereas Neuro-GPT utilized a patch size of two seconds. Similarly, context length also varied among EEG-FMs. FoME was trained using 90-second segments represented by 15 tokens. LaBraM could take up to 256 tokens as input, with the number of temporal tokens depending on the number of channels used. Neuro-GPT utilized a 32-token context window with overlapping segments, covering ~57.8 seconds of EEG. BIOT utilized 19 tokens per channel and EEGFormer utilized 12 seconds of EEG context as input.

Model scale: The number of trainable parameters (or weights) varied significantly between the ten EEG-FMs, ranging from 3.3M in BIOT to 1.7B in NeuroLM, although most models fall within the 200-500M parameter range. Some EEG-FMs, such as FoME, LaBraM, and NeuroLM, were developed in multiple scales with the same architecture, allowing users to choose a model scale according to their specific resource constraints.

4.3 Model Evaluations

Downstream task evaluations: Performance on downstream tasks post-adaptation was the primary metric used for evaluation in all the EEG-FMs. However, the clinical and non-clinical downstream tasks used for evaluation and the adaptation techniques varied significantly between them. The various datasets used for evaluation are shown in Table 2. While most EEG-FM evaluations were restricted to either scalp EEG or intracranial EEG, two models, namely FoME and BrainWave, performed evaluations on both modalities. Furthermore, most FMs utilized common adaptation techniques, such as linear probing and fine-tuning, while some FMs utilized more esoteric approaches, such as proto-type-based few-shot evaluations and instruction tuning.

Almost all EEG-FMs, except Mentality, investigated fine-tuning for downstream task evaluations, where the decoder is generally discarded and the encoder is retained for additional training. On the other hand, five EEG-FMs (i.e., Brant, BrainBERT, LaBraM, EEGFormer, and Neuro-GPT) evaluated linear probing, where the encoder is typically frozen and additional task-specific heads on top of the encoder are trained using labeled downstream data. The BrainWave model was evaluated using a prototype-based few shot learning, where class prototypes were created by averaging the latent representations of a few examples from each class and downstream classifications were performed by measuring the similarities to those prototypes in the learned latent space. Furthermore, NeuroLM, which was pretrained using an EEG-text alignment objective, was evaluated using a text prompting approach. The model was fine-tuned (instruction-tuned) using an auto-regressive prediction task utilizing EEG-text combined tokens, where the text tokens contained both class prompts and labels. Subsequently, the model was evaluated on various tasks by providing queries containing EEG tokens and prompts, for which the model predicted the class labels. In the following, we briefly summarize the evaluations performed by each EEG-FM and the results.

BrainBERT: This model was trained and evaluated on the same intracranial EEG dataset, Brain TreeBank. The downstream task focused on predicting the features of the movies subjects were watching during the EEG recording. Fine-tuning the pretrained BrainBERT model on this task substantially outperformed fully-supervised linear and multi-layer neural network models. Linear probing also achieved Area Under the Receiver Operating Characteristic Curve (AUC) values similar to the fully-supervised models.

Neuro-GPT: This model was evaluated on a single scalp EEG dataset that was not used during pretraining, where the downstream task was a 4-class motor-imagery classification. The fully-supervised baselines considered in this study include BENDR¹²⁵, SVM¹²⁶, EEGNet⁷⁴, CTCNN¹²⁷, CCNN¹²⁸, and NG-CRAM¹²⁹. When used in a supervised setting without any pretraining, this model performed similar to other supervised baselines. However, when the pretrained model was fine-tuned for the downstream task, it provided significant improvements in certain configurations. In contrast, linear probing performed worse than fully-supervised baselines.

Brant: This model was evaluated on three intracranial EEG datasets, one of which was used for pretraining. The downstream tasks evaluated include signal forecasting, imputation, and seizure detection. For all these tasks, the pretrained model was fine-tuned or linear probed for the respective task. The fully-supervised baselines with pretraining considered in this study included (RP, TS, CPC)⁷, BENDR¹²⁵, MVT¹³⁰ and BrainBERT that are designed for brain signals and CoST¹³¹, TF-C¹³², PatchTST¹³³, TS-TCC¹³⁴ that are for general time series. Fully-supervised baselines without any pretraining included, handcrafted features-based methods such as spectral power¹³⁵, rhythmicity spectrogram¹³⁶, and amplitude-integrated EEG¹³⁷ along with SEEG-Net¹³⁸. In signal forecasting and imputation tasks, fine-tuned Brant consistently outperformed several time series baselines and its own linear probing version. In the seizure detection task, both the fine-tuned and linear probed versions of Brant outperformed other supervised and EEG-FM baselines, including BrainBERT. These observations held true even in low-labeled settings.

BIOT: This model was evaluated entirely on scalp EEG datasets on various clinical tasks. The supervised baselines considered in this study included SPaRCNet¹³⁹, ContraWR¹⁴⁰, CNN-Transformer¹⁴¹, FFCL¹⁴², ST-Transformer¹⁴³. Evaluations showed that the pretrained BIOT model with fine-tuning outperformed several fully-supervised baselines in CHB-MIT seizure detection and TUAB normal/abnormal classification. Whereas, in two other tasks, namely IIIC seizure classification and TUEV event classification, both the vanilla untrained BIOT in the fully-supervised setting and the pretrained BIOT model in the fine-tuning setting outperformed all the supervised baselines.

EEGFormer: This model was evaluated on five different scalp EEG datasets, with four fully-supervised models (i.e., EEGNet⁷⁴, TCN¹⁴⁴, EEG-GNN¹⁴⁵, and GraphS4mer¹⁴⁶) and BrainBERT as baselines along with three variations

of EEGFormer with different sizes. Fine-tuned EEGFormer outperformed all baselines in all the tasks except one, where its performance was marginally lower than EEG-GNN. Their evaluations also showed that smaller version of EEGFormer demonstrated more stability in some downstream evaluations.

LaBraM: This model was evaluated on four scalp EEG datasets, two clinical (TUAB and TUEV) and two non-clinical (SEED-V and MoBI), while MoBI being the only external evaluation. The evaluations considered several supervised models, SPaRCNet¹³⁹, ContraWR¹⁴⁰, CNN-Transformer¹⁴¹, FFCL¹⁴², ST-Transformer¹⁴³, and BIOT as baselines. All variations of LaBraM (Base, Large, and Huge) with fine-tuning outperformed all the baselines in all-4 tasks, where BIOT also performed better than fully-supervised models except in MoBI. The performance gap between LaBraM and BIOT was narrower in the seizure detection task, but wider in the event classification task.

Mentality: This model was evaluated on the TUSZ seizure detection dataset, which was also used for pretraining. The evaluation compared an untrained Mentality model trained in a fully-supervised setting and a pretrained Mentality model linear probed with two linear layers, which showed that pretraining is beneficial in this task.

NeuroLM: The evaluation compared this model fine-tuned jointly on six tasks using a prompt-based tuning with seven baselines fine-tuned individually per task. The evaluations considered supervised models SPaRCNet¹³⁹, ContraWR¹⁴⁰, CNN-Transformer¹⁴¹, FFCL¹⁴², ST-Transformer¹⁴³, BIOT, and LaBraM as baselines. Their evaluations showed that joint fine-tuning using prompting is feasible and that provides reasonable performance all tasks. However, their evaluations also showed that NeuroLM did not perform as well as the LaBraM model on any of the tasks, where LaBraM was fine-tuned separately for each task. Additional evaluation using different model sizes of NeuroLM showed that performances on TUAB and TUEV were not sensitive to model size, whereas the performances on HMC and Workload tasks reduced with larger model sizes.

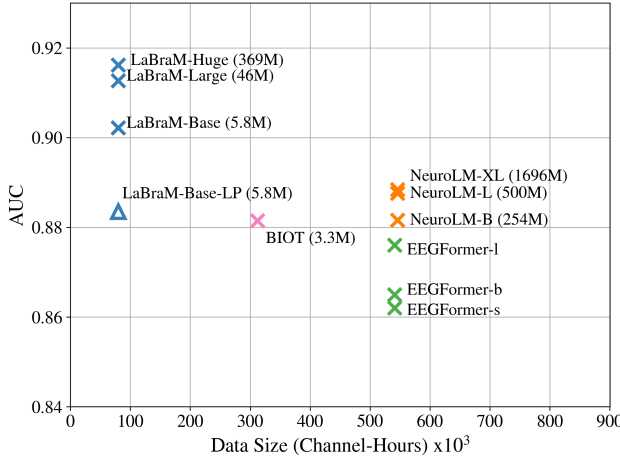
FoME: This model was evaluated on 7 tasks across 4 datasets (MAYO, FNUSA, SEED, SleepEDFx), and evaluations considered several fully-supervised models (LSTM¹⁴⁷, ConvNeXt¹⁴⁸), general time series models (PatchTST, TimesNet) and some EEG-FMs (BrainBERT, Neuro-GPT, LaBraM) as baselines. Evaluations showed that, in tasks such as emotion classification, sleep staging, and seizure detection, FoME performed competitively or better than all the baselines, whereas, its performance was significantly better in signal forecasting tasks. Interestingly, the evaluations also demonstrated that general time series models, such as PatchTST and TimesNet, perform reasonably well on tasks such as seizure detection with fine-tuning, despite not being pretrained using brain signals.

BrainWave: This model was evaluated using multiple scalp and intracranial EEG datasets and was compared against LaBraM – a scalp-EEG-FM, BrainBERT – an intracranial EEG-FM, and MOMENT¹⁴⁹ – a general time series FM. Evaluations considered different criteria, including class prototype-based few-shot classification and cross-domain transfer learning across subjects, sites, and diagnostic subtypes. Results showed that BrainWave significantly outperformed all the baselines in all settings, with an average improvement of 0.21 AUC points across 12 tasks, establishing its superiority in challenging zero-shot and OOD evaluations.

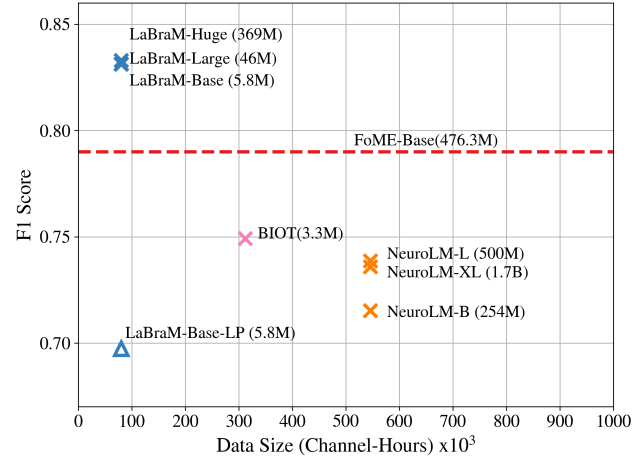
Evaluations on common tasks: We observed that two datasets, TUAB for abnormal EEG classification (two classes) and TUEV for EEG event detection (six classes), have been widely utilized for downstream evaluation. Note that both TUAB and TUEV are scalp EEG datasets derived from the larger TUH EEG corpus. In Figure 3a-3b, we compare the performances reported on some common clinical tasks. We also analyzed the impact of the pretraining data size in the x-axis. For comparison, we use AUC and F1 scores as performance metrics as they are the most commonly reported metrics for these two tasks. Linear probing results were only available in LaBraM and are indicated with a triangle in the figure. The rest of the results are based on fine-tuning experiments performed by LaBraM, NeuroLM, EEGFormer, and BIOT. We find that AUC values ranged 0.86 – 0.92 for TUAB abnormal EEG classification and F1-scores ranged 0.70 – 0.85 for TUEV event classification, highlighting a significant performance variation across models. These comparisons also suggested that the size of the pretraining data has a minimal-to-negative relation to model performance on these two tasks.

Apart from downstream task evaluations, some models performed additional evaluations focused on model interpretability, pretraining quality, and ablations. We briefly summarize those evaluations below.

Interpretability analyses: An analysis performed in BrainBERT utilized the intrinsic dimensionality (ID) measure to analyze its task-specific embeddings post-finetuning. ID is a geometric measure used to quantify the minimum number of parameters required to represent the embeddings⁶⁸. Their experiments based on a speech decoding task



(a) TUAB: normal vs. abnormal classification.



(b) TUEV: six-class event classification.

Figure 3. EEG-FM performances on TUAB and TUEV classifications. The performance of FoME in 3b is shown using a line since the pretraining data size was not available. Channel-hours are on a 10^3 scale. All scores represents fine-tuned model performance except for triangular markers that represents linear probed model performance.

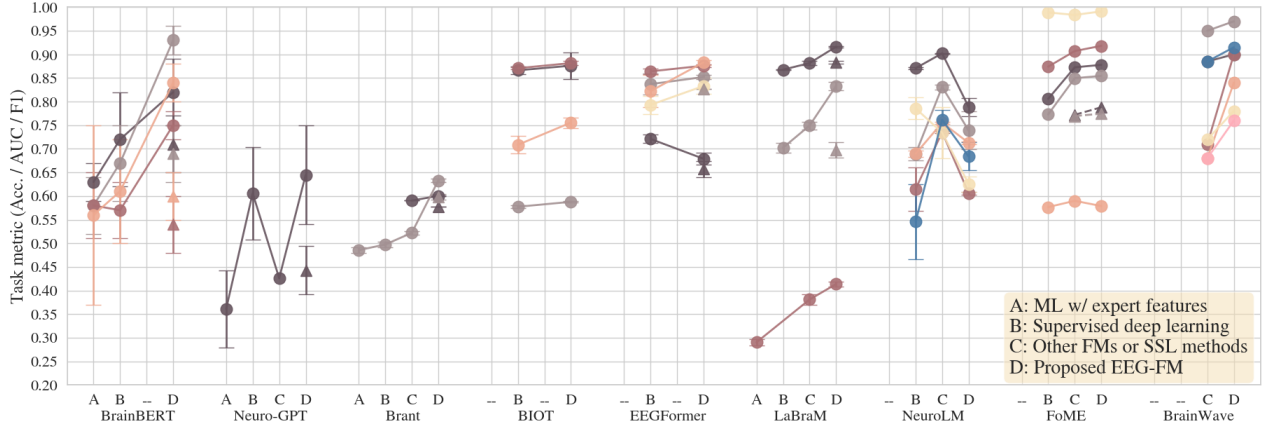
showed that electrodes within top 10th percentile of IDs mainly fall in the regions of the brain that are associated with speech. Similarly, EEGFormer, one of the three models that utilized a vector quantizer to train a neural codebook, analyzed the learned codebook to attribute parts of the input EEG data to downstream task predictions.

Pretraining quality: Some models evaluated the quality of pretraining via qualitative and quantitative assessments. Most qualitative assessments were based on visualization of the data reconstructed by the specific models, which were performed in Mentality, LaBraM, and BrainBERT. Quantitative assessments focused on reconstruction error (e.g., Mentality) and performance on forecasting and imputation tasks (e.g., Brant, FoME).

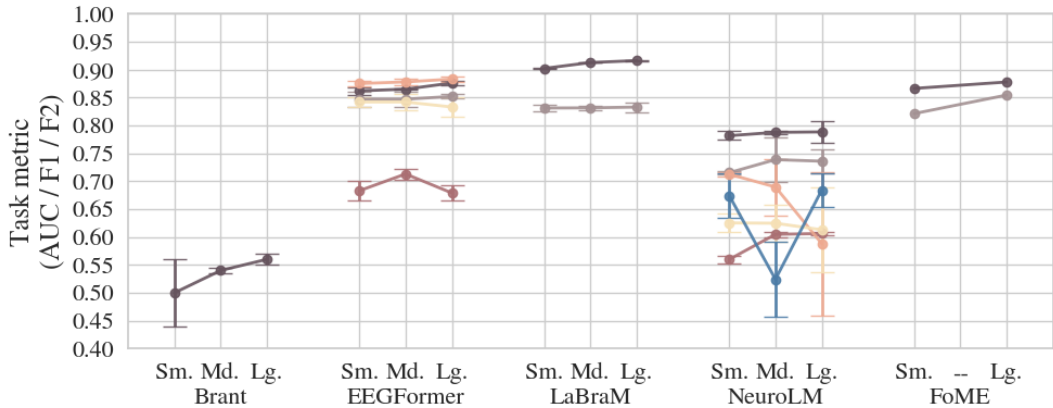
Ablations: Few models evaluated the contributions of various model components or datasets to task performance via ablations. An experiment performed in Neuro-GPT, which included a convolutional-transformer and a GPT decoder, showed that removing the GPT decoder improved downstream performance significantly. Experiments in Brant evaluated the contributions of the temporal encoding, spatial encoding, and the frequency encoding and demonstrated that while all of those components were valuable to learn EEG representations, the contributions of the temporal encoder were the highest. Similarly, LaBraM showed that the spatial embeddings are crucial for the pretraining to converge as well as to perform well in downstream evaluations after pretraining. Furthermore, LaBraM studied the effect of the codebook during pretraining by removing the neural tokenizer with traditional raw EEG (& frequency) masked reconstruction and shows that it loses performance with complex tasks such as TUEV on downstream. NeuroLM showed that different neural tokenizer training tasks (frequency vs. temporal vs. frequency & temporal reconstruction), can be beneficial for different downstream tasks. Additionally, NeuroLM studied the impact of the duration of model pretraining by fine-tuning different checkpoints, and the results were inconclusive. An experiment in BrainWave performed a data ablation by training separate models with scalp and intracranial EEG and compared the performance against joint scalp-iEEG training. Their results indicated that joint training generally improved downstream performance in all tasks, except one.

5 Key Takeaways and Research Gaps

This section presents several key observations made across the preceding comparative analyses (Section 4) and highlights the research gaps that remain. We believe that addressing these gaps would make future generations of EEG-FMs more principled in their methodology and trustworthy for scientific and clinical investigations.



(a) Impact of progressive learning paradigms (A → D) on downstream EEG classifications (○ - fine-tuning, △ - linear probing). Tasks are not comparable across studies. Shared tasks evaluated by multiple studies are shown in Figure 3.



(b) Model scaling and performance gains. Model sizes are specific to each study. ‘Sm.’ - smallest variant, ‘Md.’ - intermediate variant, ‘Lg.’ - largest variant.

Figure 4. The impact of self-supervised pretraining and model scaling on task performance. Note that downstream tasks and their performance metrics are different within and across EEG-FM studies.

5.1 Key Takeaways

Diversity of pretraining data: Several EEG-FMs (LaBraM, NeuroLM, FoME, and BrainWave) leveraged a diverse set of EEG domains spanning clinical, sleep, and task-based BCI. LaBraM’s lead in the TUAB and TUEV evaluations (Figure 3) may have emerged from its higher diversity in pretraining data compared to EEGFormer and BIOT. LaBraM also performed competitively in seizure classification tasks on the MAYO and FNUSA datasets as reported in FoME’s evaluations. Note that LaBraM was pretrained on significantly fewer channel-hours of scalp EEG data and while TUAB and TUEV evaluations are both in-distribution assessments, MAYO-FNUSA evaluations are both intracranial EEG datasets. The mixed use of scalp and intracranial EEG, as done in FoME and BrainWave, can be considered as another form of data diversity. Using data ablations (scalp EEG vs. iEEG), BrainWave demonstrated that joint pretraining (scalp EEG + iEEG) leads to a boost in downstream task performance and transfer performance to unseen data types (electrocardiograms). Overall, the notion of data diversity, perhaps in conjunction with data volume, may influence the performance, generalizability, and transferability of EEG-FMs.

Minimal data preprocessing: Most EEG-FMs perform minimal and simple data preprocessing steps, namely filtering and resampling, to standardize EEGs from various sources. Notably, the removal of noise-related outliers, suppression of EEG artifacts, artifactual EEG components, and site-related harmonization were not explicitly pursued. Moreover, data normalization strategies that produce training-ready samples were not sufficiently described in most studies. It remains unclear whether or how various offline data handling strategies impact EEG-FM pretraining and

downstream task performance, particularly with OOD test data.

Multivariate time series EEG representation: All but four EEG-FMs utilized the native multivariate time series representation of EEG, while two models utilized the spectral representations. Two other models combined time-series and spectral representations as input, while the remaining two models exclusively adopted time-frequency representations. Subsequently, the respective EEG inputs were positionally encoded with their spatial and temporal order. Due to a lack of shared downstream evaluations and ablation studies, it is difficult to assess the relative contributions of different EEG input representations and spatial positional encoding schemes. Furthermore, the context length of the EEG-FMs did not exceed 90 seconds (FoME), and as such, they may struggle to capture long-range EEG patterns, relationships, or dependencies.

Temporal sequence modeling: Sequence-based transformer blocks were the primary workhorse of representation learning in most EEG-FMs, with the exception of Mentality, which was based on a Mamba-based architecture. A few models (NeuroLM, Neuro-GPT) utilized convolutions to capture low-level morphological features of time-domain EEG. However, the modeling of spatial EEG relationships was either ignored or limited to the positional encoding step. BrainWave, a notable exception in this trend, integrated a spatial attention mechanism. Supporting such emphasis on temporal modeling, the ablation experiments in Brant showed that their temporal encoder provided the largest contribution to downstream task performance, compared to the spatial encoder and frequency encoding.

Pretraining using masked reconstruction: Reconstruction of masked temporal EEG sequences was the predominant EEG-FM pretraining paradigm, albeit with varying strategies for masking of sequence tokens/patches. Despite its origins in vision and language domains, this SSL strategy seemingly holds merit in the EEG domain. However, the generalizability of representations learned during pretraining is generally unclear since most evaluations were performed after fine-tuning on downstream data. In addition, several studies (LaBraM, NeuroLM, EEGFormer) employed a learned discrete neural codebook to further facilitate the pretraining process. In auxiliary efforts, this codebook can support interpretability (EEGFormer) and interface with discrete language vocabularies (NeuroLM).

Limited model evaluations: Task performance after fine-tuning was the primary paradigm of EEG-FM evaluation. However, in half the reviewed studies (BrainBERT, Brant, Mentality, NeuroLM, and FoME), the downstream evaluation datasets were already utilized for FM pretraining, i.e., the evaluations were in-sample. Although several studies conducted external evaluations on unseen datasets, BrainWave is the only study that performed truly OOD task evaluations, i.e., without fine-tuning the model on the evaluation set. Direct model rankings beyond the TUAB and TUEV tasks are difficult to determine due to heterogeneous selections of downstream tasks across most EEG-FMs (see Table 2). Even when considering the TUAB and TUEV tasks, only four out of the ten EEG-FMs can be ranked, as depicted on the y-axis in Figures 3a and 3b, respectively. In addition, linear probing or few-shot evaluations were rarely reported (see Fig. 4a). Overall, the number of meaningful EEG classification tasks evaluated in each study ranged from 1 (Mentality) to 12 (BrainWave), with most studies evaluating proposed EEG-FMs on at most 5 tasks. Overall, the universality and robustness of EEG-FMs has not been convincingly demonstrated in most studies, with BrainWave being a notable exception.

Model scaling and task performance: In Figure 4b, we analyze the impact of model scaling on task performance using studies with at least two model variants. Each line plot indicates a specific downstream task and the x-axis shows model variants, which were typically classified as small, intermediate, and large. Some marginal improvements can be observed for certain tasks and models, although these variants were developed with a fixed amount of pretraining data and were evaluated within study-specific experimental and methodological contexts. Notably, LaBraM investigated the combined effects of pretraining data and model scale on downstream TUAB/TUEV classifications. Overall, it is unclear whether a clear and strong trend exists with model scaling, especially within the current EEG-FM parameter regime ranging from 3.3M (BIOT) to 1.7B (NeuroLM, largest variant).

Performance of general-purpose time series models: Interestingly, we observed that general time series foundation models, such as TimesNet¹⁵⁰, performed reasonably well on several EEG tasks post-fine-tuning, and sometimes outperformed EEG-FMs (e.g., sleep-stage classification in FoME). Additionally, experiments in BrainWave show that, a time series FM – MOMENT¹⁴⁹ – outperformed EEG-FMs in specific tasks, such as seizure detection. Experiments in Brant show that general time series architectures, such as PatchTST¹⁵¹ and CoST¹³¹, perform relatively better in some tasks, such as short/long term signal forecasting and imputation, respectively, than some

EEG-specific architectures. These findings highlight that certain EEG tasks could be tackled using general time series architectures or FMs without any EEG-specific inductive biases.

Data scaling and task performance: The trend along x-axis of Figures 3a and 3b suggests that scaling up pretraining data may lead to worse downstream task performance, even with significant model scale up (e.g., LaBraM vs. EEGFormer/NeuroLM). Notably, LaBraM demonstrated that effects of pretraining data scaling on TUAB and TUEV classifications are sharpest under ~ 1000 hours of data and begin to plateau thereafter. Overall, the evidence for data scaling is weak, if any, based on the limited shared tasks and models evaluated thus far.

Advance over other feature paradigms: In Figure 4a, we compare progressive feature extraction paradigms (expert features with classical ML, data-driven supervised DL features, self-supervised DL features, and proposed EEG-FMs) on various tasks. In a majority of tasks, fine-tuned EEG-FMs ('D') provided at least some improvement, if not drastic, over previous DL baselines and FMs ('B' and 'C', respectively). Linear probing results reported in EEG-FMs, however, were relatively worse in comparison. Fine-tuned EEG-FMs showed substantial improvements over classical ML models with expert features ('A'), although such assessments were presented only in four studies.

5.2 Current Research Gaps

Data and model scaling: The scaling up of data and models is a defining principle of foundation modeling. However, empirical evidence of scaling in EEG-FMs has been either weak, limited, or inconclusive. Investigations that scale up data volume (channel-hours), model size (trainable parameters), and evaluate on an expansive set of downstream tasks are lacking in current EEG-FMs, particularly at sufficiently large scales where effects are clear and discernible.

Preprocessing and normalization effects: EEG datasets can require significant offline preprocessing to manage data quality and suppress artifacts. Since current studies perform minimal processing, it is unclear whether or to what extent data outliers and noise impact EEG-FM pretraining and task performance. Even clean EEG datasets require careful consideration of normalization strategies as EEG can vary across channels, subjects, and acquisition sites⁶. The choice of input representation can further complicate decisions related to preprocessing and normalization. As such, there is a need to better understand the impact of these choices on downstream EEG-FM modeling.

Model ablations: EEG-FM design involves two significant choices: the input representations and the internal architectural components. However, the lack of systematic exploration of the effects of these choices in existing EEG-FM literature prevents principled choices in EEG-FM design. The relative merits of time-domain and time-frequency domain inputs remain unclear, although both appear to be effective. The contributions of positional encoding schemes, both temporal and spatial, can be better understood. Similarly, the effects of time-domain and channel-domain spatial attention mechanisms on learned patterns remain poorly understood.

Long temporal context and spatial modeling: Slow variations over long timescales can exist in multi-day intracranial EEGs or multi-hour sleep-related EEG recordings¹⁵². However, current EEG-FMs can only process patterns within sequences of 90 seconds or less. There is a need for solutions that expand the effective context length of EEG-FMs. Moreover, the explicit modeling of spatial or inter-channel relationships and their contributions relative to temporal modeling requires further investigation.

Quality of pretraining strategy: EEG-FM linear probing evaluations reported by some studies have performed significantly worse than fine-tuned versions and other baselines in several instances (see Figure 4a). However, some gains can be seen when FMs are fine-tuned on task data compared to fully-supervised training on the same data. This contrasting observation casts doubt on the inherent/intrinsic quality of the representations learned via self-supervision in EEG-FMs. Further investigations into the effects of SSL pretraining on downstream evaluations are needed to fully understand the extent of transferability achieved through SSL. Beyond the SSL strategy itself, the effects of data diversity, data volume, and model scale on the quality of EEG-FM pretraining remain unknown.

Practically relevant evaluations and metrics: Current fine-tuning evaluations are limited in their capacity to assess the real-world practical utility of EEG-FMs. There is a need to adopt evaluation schemes and task metrics that capture the reality of EEG research and clinical use. Zero-shot evaluations are required for off-the-shelf EEG-FM usage for novel, unseen tasks. Few-shot or low-label performance can assess how efficiently EEG-FMs can leverage EEG labels that are typically expensive and laborious to collect. Out-of-distribution performance, especially without fine-tuning, on a known task can help understand EEG-FM robustness to the idiosyncratic cross-subject and cross-site

variability of EEG. Finally, application-specific metrics, such as false positives per hour for seizure detection, and comparisons with expert EEG feature baselines can further clarify the real-world utility of EEG-FMs.

Standardized benchmarking tasks: The comparative analysis revealed significant heterogeneity in the tasks selected for EEG-FM evaluation (see Table 2). The lack of common tasks across EEG-FM evaluations makes it challenging to understand the state-of-the-art, and highlights a need to identify a common core set of evaluations for future EEG-FM evaluations. This set must cover multiple task types and include both classifications and regressions, with dense (one label for the entire EEG recording) and sparse (one label for each EEG segment) labels. Additionally, the tasks must be challenging for previous generations of EEG-DL models with ample room for improvement, unlike TUAB, where performance may have already saturated (85-87% accuracy) with traditional approaches¹⁵³.

Trustworthy modeling: None of the reviewed EEG-FMs focused on model explainability or interpretability, which remain key requirements for data-driven modeling in high-risk and expert-centric domains such as medicine. Studies that demystify the EEG-FM black box are needed to gain insight into knowledge learned by EEG-FMs (EEG patterns, dependencies, relationships) through pretraining and the practical robustness of their decision-making process for downstream applications. Connections to known patterns of brain physiology or pathology may be necessary to make EEG-FMs trustworthy in the eyes of expert users.

6 Proposed Future Directions

From a time series perspective, EEG signals are distinct from general signals or sequences due to their unbounded real-valued amplitude, non-linearity¹⁵⁴, non-stationarity¹⁵⁴, and 1/f spectral characteristics¹⁵⁵. These peculiarities would suggest that foundation modeling for EEG signals requires domain-specific approaches. Indeed, we have cultivated an EEG-centric, domain-sensitive ethos throughout this review. However, counter-intuitively, EEG-FMs have enjoyed some success in drawing from vision and language domains in their adoption of sequence patching and transformer architecture design (transformer⁴⁵, vision transformer⁶²), masked reconstruction-based SSL (masked autoencoders¹²⁴), and discrete neural codebooks (VQ-VAE¹²³, BEiT v2¹⁵⁶). Moreover, time series FMs pretrained on generic, non-neural time series have performed similarly to EEG-FMs on certain EEG tasks. Therefore, it is likely that future EEG-FMs could benefit from embracing both domain-specific insights and innovations from external data domains. These domains may be semantically distant to EEG, such as vision and natural language, or loosely related, such as non-neural time series, audio, speech, or other biosignals. Below, we outline the future research directions that we believe could support meaningful and sustained progress in the EEG-FM research domain. As illustrated in Figure 5, these recommendations are organized under three broad themes of development spanning benchmarks and software tools, technical advances, and real-world applications. These suggestions build upon the research gaps identified earlier and provide additional guidance for advancing and accelerating EEG-FM research and adoption.

6.1 Benchmarks and Tools

Benchmarking against prevailing feature paradigms: Quantitative EEG research currently employs two ML feature paradigms: expert-crafted EEG features and task-specific supervised features. As such, data-driven self-supervised features, such as those provided by EEG-FMs, remain in their infancy. Therefore, to establish a compelling case for EEG-FM adoption, studies proposing novel EEG-FMs should evaluate against the prevailing feature paradigms. In doing so, statistical tests of superior performance must be presented wherever necessary, and identical subject data splits must be used to prevent the influence of inter-subject EEG variability.

Ranking EEG-FMs in global EEG competitions: Novel EEG-FM methodology can leverage international predictive modeling competitions to establish real-world performance and utility, as those competitions can highlight the most significant empirical challenges or milestones within the field. Such competitions have already been developed for time series¹⁵⁷, electrocardiograms¹⁵⁸, and speech¹⁵⁹ domains. Notably, within the EEG domain, previous competitions have highlighted issues with transfer learning under distribution shifts¹⁶⁰, abnormality detection¹⁶¹, coma prognosis¹⁶², and seizure detection¹⁶³. The creation of new EEG competitions also incentivizes the public release of expertly curated and annotated EEG datasets that can further boost EEG-FM research.

Frictionless software: Several software modifications and code debugging are required to run the currently available EEG-FMs. The deep technical nature of EEG-FMs and the computing skills required to run these models present a

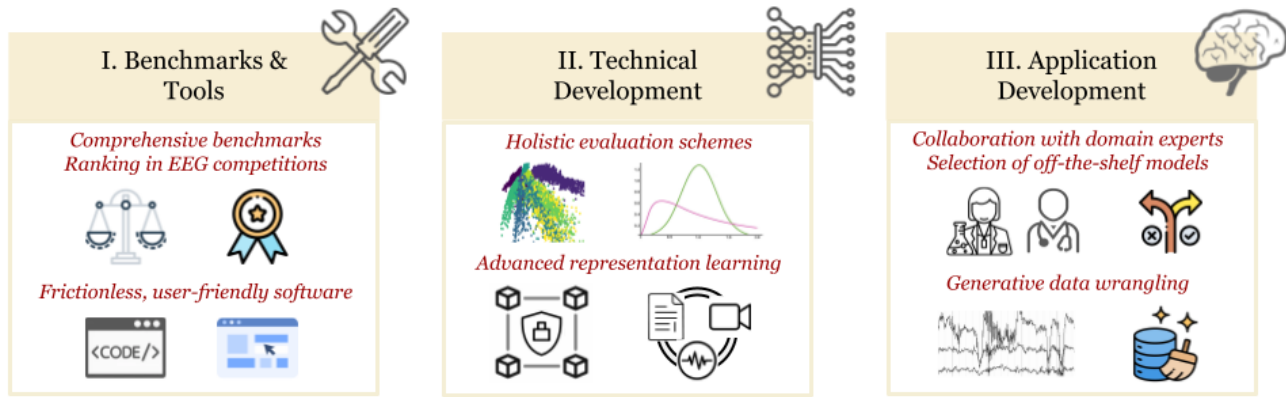


Figure 5. Illustration of future directions along three key developmental axes; benchmarks and tools, technical modeling, and applications. I. Future EEG-FMs can be compared against prevailing feature paradigms and participate in EEG challenges to establish their real-world utility. Frictionless and user-friendly software tools are needed to quickly adopt and experiment with off-the-shelf models. II. Holistic evaluation frameworks that test embedding space semantics, robustness, and transfer efficiency can meaningfully track the state-of-the-art. Advanced representation learning techniques, such as federated or multi-modal learning, can enhance large-scale pretraining. III. Collaborations with domain experts can inspire novel EEG-FM applications. Although current applications are largely discriminative, future applications could be generative in nature.

considerable entry barrier to non-technical or non-computational researchers. It will be necessary for future studies to ensure that EEG-FMs can be used as off-the-shelf feature extraction tools, with no technical modifications required. Graphical software for plug-and-play EEG-FM analytics, such as simple binary classifications, can greatly increase real-world EEG-FM adoption, testing, and experimentation. Encouragingly, a mature ecosystem for large-scale EEG analytics already exists in Python^{164–166} and can support the development of frictionless EEG-FM software.

6.2 Technical Development

Holistic evaluation schemes: Evaluating EEG-FMs based on their task performance on publicly available EEG datasets/tasks is insufficient to measure their real-world readiness. Novel evaluation schemes can be designed to assess the computational costs, semantic EEG-FM embedding quality, transfer efficiency, and robustness to real-world EEG variability and noise sources. The development of such evaluation schemes can leverage the wealth of expert knowledge already available within the EEG domain.

Privacy-preserving learning: EEG datasets required for large-scale EEG-FM pretraining can be siloed due to patient privacy and legal concerns. Research collaborations involving multiple clinical sites can utilize federated learning¹⁶⁷ techniques to train EEG-FMs without requiring centralized data access or sharing. Such techniques may also support the development of personalized patient-specific models.

Multi-modal learning: Latent representations learned during pretraining may benefit from cross-modal supervision from text reports, video recordings, or other biosignals like electrocardiograms. Some of these modalities are jointly recorded with EEGs in many clinical and scientific recording settings. Notably, downstream applications can reap the performance benefits of cross/multi-modal pretraining without requiring those modalities during evaluation.

Reasoning and agentic capabilities: Future EEG-FMs could be fine-tuned to mimic expert reasoning processes, adhere to expert grading criteria¹⁶⁸ or instructions, and autonomously retrieve relevant evidence from knowledge bases. Augmented healthcare workflows could utilize insights from a specialized EEG agent, along with other modality-specific clinical data agents, to inform clinical decisions.

Scaling down task-specific EEG-FMs: FMs may require model parameter scaling to obtain superior pretrained features. However, large EEG-FMs may not be suitable for applications involving streaming EEG data, real-time EEG processing, or deployment in resource-constrained settings, such as brain-computer interfaces, medical devices, and clinical environments. In such contexts, model distillation¹⁶⁹, pruning¹⁷⁰, or quantization¹⁷¹ techniques can

deliver smaller, computationally inexpensive inference-only models that maintain high task performance.

6.3 Application Development

Cross- and inter-disciplinary collaboration: The technical development of EEG-FMs should involve close collaboration with scientific and clinical domain experts. Such collaborations can productively constrain and inspire novel modeling decisions, identify novel research gaps, establish clear criteria for real-world success or progress, and facilitate EEG-FM experimentation among niche application-specific audiences.

Model cards to guide EEG-FM selection: The availability of multiple EEG-FMs, each purportedly an off-the-shelf tool, poses a practical dilemma for domain experts who must make a principled selection for their research. Comprehensive comparisons of all available options may not be feasible in discovery-based research. The release of model cards¹⁷² that summarize an EEG-FM's functional strengths and weaknesses, inherent or dominant inductive biases, compute requirements, and evaluation scope and rankings could inform the model selection process.

Generative applications: Existing EEG-FMs have primarily focused on learning latent, low-dimensional encodings of raw EEG data. Future studies could explore generative EEG-FM applications by increasing the representational capacity of the EEG decoder. Generative EEG-FMs may be useful in EEG data wrangling tasks, including data denoising, repairing corrupted segments, and imputing missing data, among others. Controllable EEG generation may be applied towards data augmentation within EEG representation learning pipelines.

7 Conclusion

The promise of foundation models, in principle, lies in effective and robust feature learning, feature re-usability, and label efficiency. Our critical analysis of the state-of-the-art EEG-FMs indicates that the first-generation EEG-FMs, inspired by their counterparts in the mainstream vision and language domains, have made early, moderate strides in realizing this promise for the EEG domain. However, to develop universal, robust, and general-purpose EEG feature extractors, next-generation EEG-FMs must prioritize substantial scaling efforts, principled and trustworthy self-supervised representation learning, and practically relevant evaluations. In addition to technical modeling, we believe that future research should also pursue the collaborative development of meaningful EEG benchmarks, applications, and model evaluation schemes that can measurably track the real-world readiness and impact of EEG-FMs. With sustained efforts in these directions, EEG-FMs are poised to advance scientific research, brain-computer interfaces, and clinical decision support systems.

8 Acknowledgments

We would like to thank Mario Serrafero and Saeid Cheshmi for fruitful discussions on foundation modeling.

9 Funding

This study was supported in part by the Mayo Clinic & Illinois Alliance Fellowship for Technology-based Healthcare Research, the Edward Heiken Interdisciplinary Health Sciences Institute Fund, and NSF grants IIS-2105233, IIS-2344731, and IIS-2337909.

References

1. Mushtaq, F. *et al.* One hundred years of EEG for brain and behaviour research. *Nat. Hum. Behav.* **8**, 1437–1443, DOI: [10.1038/s41562-024-01941-5](https://doi.org/10.1038/s41562-024-01941-5) (2024).
2. Diniz, J. B. C. *et al.* Advancing epilepsy diagnosis: A meta-analysis of artificial intelligence approaches for interictal epileptiform discharge detection. *Seizure: Eur. J. Epilepsy* **122**, 80–86 (2024).
3. Roy, Y. *et al.* Deep learning-based electroencephalography analysis: A systematic review. *J. Neural Eng.* **16**, 051001, DOI: [10.1088/1741-2552/ab260c](https://doi.org/10.1088/1741-2552/ab260c) (2019).
4. Craik, A., He, Y. & Contreras-Vidal, J. L. Deep learning for electroencephalogram (EEG) classification tasks: A review. *J. Neural Eng.* **16**, 031001, DOI: [10.1088/1741-2552/ab0ab5](https://doi.org/10.1088/1741-2552/ab0ab5) (2019).
5. Obeid, I. & Picone, J. The temple university hospital eeg data corpus. *Front. neuroscience* **10**, 196 (2016).
6. Wagh, N., Wei, J., Rawal, S., Berry, B. M. & Varatharajah, Y. Evaluating latent space robustness and uncertainty of eeg-ml models under realistic distribution shifts. *Adv. Neural Inf. Process. Syst.* **35**, 21142–21156 (2022).
7. Banville, H., Chehab, O., Hyvärinen, A., Engemann, D.-A. & Gramfort, A. Uncovering the structure of clinical eeg signals with self-supervised learning. *J. Neural Eng.* **18**, 046020 (2021).
8. Bommasani, R. *et al.* On the opportunities and risks of foundation models. *arXiv preprint arXiv:2108.07258* (2021).
9. Yuan, L. *et al.* Florence: A new foundation model for computer vision. *arXiv preprint arXiv:2111.11432* (2021).
10. Kirillov, A. *et al.* Segment anything. In *Proceedings of the IEEE/CVF international conference on computer vision*, 4015–4026 (2023).
11. Radford, A. *et al.* Learning transferable visual models from natural language supervision. In *International conference on machine learning*, 8748–8763 (PMLR, 2021).
12. Chowdhery, A. *et al.* Palm: Scaling language modeling with pathways. *J. Mach. Learn. Res.* **24**, 1–113 (2023).
13. Touvron, H. *et al.* Llama: Open and efficient foundation language models. *arXiv preprint arXiv:2302.13971* (2023).
14. Achiam, J. *et al.* Gpt-4 technical report. *arXiv preprint arXiv:2303.08774* (2023).
15. Wang, C. *et al.* Brainbert: Self-supervised representation learning for intracranial recordings. *arXiv preprint arXiv:2302.14367* (2023).
16. Cui, W. *et al.* Neuro-gpt: Towards a foundation model for eeg. In *2024 IEEE International Symposium on Biomedical Imaging (ISBI)*, 1–5 (IEEE, 2024).
17. Zhang, D. *et al.* Brant: Foundation model for intracranial neural signal. *Adv. Neural Inf. Process. Syst.* **36** (2024).
18. Yang, C., Westover, M. & Sun, J. Biot: Biosignal transformer for cross-data learning in the wild. *Adv. Neural Inf. Process. Syst.* **36** (2024).
19. Chen, Y. *et al.* Eegformer: Towards transferable and interpretable large-scale eeg foundation model. *arXiv preprint arXiv:2401.10278* (2024).
20. Jiang, W.-B., Zhao, L.-M. & Lu, B.-L. Large brain model for learning generic representations with tremendous eeg data in bci (2024). ArXiv:2405.18765 [cs].
21. Panchavati, S. & Speier, W. Mentality. In *ICLR 2024 Workshop on Learning from Time Series For Health* (2024).
22. Jiang, W.-B., Wang, Y., Lu, B.-L. & Li, D. NeuroLM: A Universal Multi-task Foundation Model for Bridging the Gap between Language and EEG Signals, DOI: [10.48550/arXiv.2409.00101](https://doi.org/10.48550/arXiv.2409.00101) (2024). ArXiv:2409.00101 [cs, eess].

23. Shi, E. *et al.* FoME: A Foundation Model for EEG using Adaptive Temporal-Lateral Attention Scaling (2024). ArXiv:2409.12454 [cs, eess].

24. Yuan, Z. *et al.* Brainwave: A brain signal foundation model for clinical applications (2024). [2402.10251](#).

25. Tatum, W. O. *et al.* Clinical utility of eeg in diagnosing and monitoring epilepsy in adults. *Clin. Neurophysiol.* **129**, 1056–1082 (2018).

26. da Silva, F. L. Eeg and meg: relevance to neuroscience. *Neuron* **80**, 1112–1128 (2013).

27. Värbu, K., Muhammad, N. & Muhammad, Y. Past, present, and future of eeg-based bci applications. *Sensors* **22**, 3331 (2022).

28. Buzsáki, G., Anastassiou, C. A. & Koch, C. The origin of extracellular fields and currents—eeg, ecog, lfp and spikes. *Nat. reviews neuroscience* **13**, 407–420 (2012).

29. Brunner, C., Billinger, M., Seeber, M., Mullen, T. R. & Makeig, S. Volume conduction influences scalp-based connectivity estimates. *Front. computational neuroscience* **10**, 121 (2016).

30. Petroff, O. A., Spencer, D. D., Goncharova, I. I. & Zaveri, H. P. A comparison of the power spectral density of scalp eeg and subjacent electrocorticograms. *Clin. Neurophysiol.* **127**, 1108–1112 (2016).

31. Klimesch, W. Memory processes, brain oscillations and eeg synchronization. *Int. journal psychophysiology* **24**, 61–100 (1996).

32. Oken, B. S., Salinsky, M. C. & Elsas, S.-M. Vigilance, alertness, or sustained attention: physiological basis and measurement. *Clin. neurophysiology* **117**, 1885–1901 (2006).

33. Perinelli, A., Asseconti, S., Tagliabue, C. F. & Mazza, V. Power shift and connectivity changes in healthy aging during resting-state eeg. *NeuroImage* **256**, 119247 (2022).

34. Amin, U., Nascimento, F. A., Karakis, I., Schomer, D. & Benbadis, S. R. Normal variants and artifacts: importance in eeg interpretation. *Epileptic disorders* **25**, 591–648 (2023).

35. Blume, W. T. Drug effects on eeg. *J. Clin. Neurophysiol.* **23**, 306–311 (2006).

36. Li, B., Cheng, T. & Guo, Z. A review of eeg acquisition, processing and application. In *Journal of Physics: Conference Series*, vol. 1907, 012045 (IOP Publishing, 2021).

37. Céspedes-Villar, Y., Martinez-Vargas, J. D. & Castellanos-Dominguez, G. Influence of patient-specific head modeling on eeg source imaging. *Comput. Math. Methods Medicine* **2020**, 5076865 (2020).

38. Smit, D. J., Boomsma, D. I., Schnack, H. G., Pol, H. E. H. & de Geus, E. J. Individual differences in eeg spectral power reflect genetic variance in gray and white matter volumes. *Twin research human genetics* **15**, 384–392 (2012).

39. Gao, R., Peterson, E. J. & Voytek, B. Inferring synaptic excitation/inhibition balance from field potentials. *NeuroImage* **158**, 70–78 (2017).

40. Tatum IV, W. O. *Handbook of EEG interpretation* (Springer Publishing Company, 2021).

41. Popa, L. L., Dragos, H., Panteleimon, C., Rosu, O. V. & Strilciuc, S. The role of quantitative eeg in the diagnosis of neuropsychiatric disorders. *J. medicine life* **13**, 8 (2020).

42. Roy, Y. *et al.* Deep learning-based electroencephalography analysis: a systematic review. *J. neural engineering* **16**, 051001 (2019).

43. Neumann, O. *et al.* Smart data representations: impact on the accuracy of deep neural networks. In *Proceedings 31 workshop computational intelligence*, 113–130 (2021).

44. Michel, C. M. & Brunet, D. Eeg source imaging: a practical review of the analysis steps. *Front. neurology* **10**, 325 (2019).

45. Vaswani, A. *et al.* Attention is all you need. *Adv. neural information processing systems* **30** (2017).

46. Wu, H. *et al.* Cvt: Introducing convolutions to vision transformers. In *Proceedings of the IEEE/CVF international conference on computer vision*, 22–31 (2021).

47. Ericsson, L., Gouk, H., Loy, C. C. & Hospedales, T. M. Self-supervised representation learning: Introduction, advances, and challenges. *IEEE Signal Process. Mag.* **39**, 42–62 (2022).

48. Chen, T., Kornblith, S., Norouzi, M. & Hinton, G. A simple framework for contrastive learning of visual representations. In *International conference on machine learning*, 1597–1607 (PMLR, 2020).

49. Zhang, C., Zhang, C., Song, J., Yi, J. S. K. & Kweon, I. S. A survey on masked autoencoder for visual self-supervised learning. In *IJCAI*, 6805–6813 (2023).

50. Wagh, N. *et al.* Domain-guided self-supervision of eeg data improves downstream classification performance and generalizability. In *Machine Learning for Health*, 130–142 (PMLR, 2021).

51. Thrun, S. & Pratt, L. Learning to learn: Introduction and overview. In *Learning to learn*, 3–17 (Springer, 1998).

52. Kumar, A., Raghunathan, A., Jones, R., Ma, T. & Liang, P. Fine-tuning can distort pretrained features and underperform out-of-distribution. *arXiv preprint arXiv:2202.10054* (2022).

53. Sun, C., Shrivastava, A., Singh, S. & Gupta, A. Revisiting unreasonable effectiveness of data in deep learning era. In *Proceedings of the IEEE international conference on computer vision*, 843–852 (2017).

54. Dehghani, M. *et al.* Scaling vision transformers to 22 billion parameters. In *International conference on machine learning*, 7480–7512 (PMLR, 2023).

55. Kaplan, J. *et al.* Scaling laws for neural language models. *arXiv preprint arXiv:2001.08361* (2020).

56. Yao, Q. *et al.* Towards neural scaling laws for time series foundation models. *arXiv preprint arXiv:2410.12360* (2024).

57. Isik, B. *et al.* Scaling laws for downstream task performance of large language models. In *ICLR 2024 Workshop on Mathematical and Empirical Understanding of Foundation Models* (2024).

58. Edwards, T. D., Alvey, J., Alsing, J., Nguyen, N. H. & Wandelt, B. D. Scaling-laws for large time-series models. *arXiv preprint arXiv:2405.13867* (2024).

59. Rosenfeld, J. S., Rosenfeld, A., Belinkov, Y. & Shavit, N. A constructive prediction of the generalization error across scales. *arXiv preprint arXiv:1909.12673* (2019).

60. Oquab, M. *et al.* Dinov2: Learning robust visual features without supervision. *arXiv preprint arXiv:2304.07193* (2023).

61. Wenzek, G. *et al.* Ccnet: Extracting high quality monolingual datasets from web crawl data. *arXiv preprint arXiv:1911.00359* (2019).

62. Dosovitskiy, A. *et al.* An image is worth 16x16 words: Transformers for image recognition at scale. *arXiv preprint arXiv:2010.11929* (2020).

63. Thapa, R. *et al.* Sleepfm: Multi-modal representation learning for sleep across ecg, eeg and respiratory signals. In *AAAI 2024 Spring Symposium on Clinical Foundation Models* (2024).

64. van Gorp, H. *et al.* A generative foundation model for five-class sleep staging with arbitrary sensor input. *arXiv preprint arXiv:2408.15253* (2024).

65. Devlin, J., Chang, M.-W., Lee, K. & Toutanova, K. Bert: Pre-training of deep bidirectional transformers for language understanding. In *Proceedings of the 2019 conference of the North American chapter of the association for computational linguistics: human language technologies, volume 1 (long and short papers)*, 4171–4186 (2019).

66. Gabor, D. Theory of communication. part 1: The analysis of information. *J. Inst. Electr. Eng. III: radio communication engineering* **93**, 429–441 (1946).

67. Moca, V. V., Bârzan, H., Nagy-Dăbâcan, A. & Mureşan, R. C. Time-frequency super-resolution with superlets. *Nat. communications* **12**, 337 (2021).

68. Ansuini, A., Laio, A., Macke, J. H. & Zoccolan, D. Intrinsic dimension of data representations in deep neural networks. *Adv. Neural Inf. Process. Syst.* **32** (2019).

69. Radford, A. *et al.* Language models are unsupervised multitask learners. *OpenAI blog* **1**, 9 (2019).

70. Mosher, J. C., Leahy, R. M. & Lewis, P. S. Eeg and meg: forward solutions for inverse methods. *IEEE Transactions on biomedical engineering* **46**, 245–259 (2002).

71. Gu, A. & Dao, T. Mamba: Linear-time sequence modeling with selective state spaces. *arXiv preprint arXiv:2312.00752* (2023).

72. Goel, K., Gu, A., Donahue, C. & Ré, C. It's raw! audio generation with state-space models. In *International conference on machine learning*, 7616–7633 (PMLR, 2022).

73. Ronneberger, O., Fischer, P. & Brox, T. U-net: Convolutional networks for biomedical image segmentation. In *Medical image computing and computer-assisted intervention–MICCAI 2015: 18th international conference, Munich, Germany, October 5-9, 2015, proceedings, part III* 18, 234–241 (Springer, 2015).

74. Lawhern, V. J. *et al.* Eegnet: a compact convolutional neural network for eeg-based brain–computer interfaces. *J. neural engineering* **15**, 056013 (2018).

75. Guttag, J. Chb-mit scalp eeg database (version 1.0. 0). *PhysioNet* (2010).

76. Zhang, G.-Q. *et al.* The national sleep research resource: towards a sleep data commons. *J. Am. Med. Informatics Assoc.* **25**, 1351–1358 (2018).

77. Kemp, B., Zwinderman, A. H., Tuk, B., Kamphuisen, H. A. & Oberye, J. J. Analysis of a sleep-dependent neuronal feedback loop: the slow-wave microcontinuity of the eeg. *IEEE Transactions on Biomed. Eng.* **47**, 1185–1194 (2000).

78. Terzano, M. G. *et al.* Atlas, rules, and recording techniques for the scoring of cyclic alternating pattern (cap) in human sleep. *Sleep medicine* **2**, 537–554 (2001).

79. Nejedly, P. *et al.* Multicenter intracranial EEG dataset for classification of graphoelements and artifactual signals. *Sci. Data* **7**, 179, DOI: [10.1038/s41597-020-0532-5](https://doi.org/10.1038/s41597-020-0532-5) (2020). Publisher: Nature Publishing Group.

80. Wang, C. *et al.* Brain treebank: Large-scale intracranial recordings from naturalistic language stimuli. *Adv. Neural Inf. Process. Syst.* **37**, 96505–96540 (2024).

81. van Blooij, D. *et al.* "ccep ecog dataset across age 4-51", DOI: [doi:10.18112/openneuro.ds004080.v1.2.4](https://doi.org/10.18112/openneuro.ds004080.v1.2.4) (2023).

82. Grossmann, A. & Morlet, J. Decomposition of hardy functions into square integrable wavelets of constant shape. *SIAM journal on mathematical analysis* **15**, 723–736 (1984).

83. Obeid, I. & Picone, J. The temple university hospital eeg data corpus. *Front. neuroscience* **10**, 196 (2016).

84. Detti, P., Vatti, G. & Zabalo Manrique de Lara, G. Eeg synchronization analysis for seizure prediction: A study on data of noninvasive recordings. *Processes* **8**, 846 (2020).

85. Quan, S. F. *et al.* The sleep heart health study: design, rationale, and methods. *Sleep* **20**, 1077–1085 (1997).

86. Alvarez-Estevez, D. & Rijsman, R. M. Inter-database validation of a deep learning approach for automatic sleep scoring. *PloS one* **16**, e0256111 (2021).

87. Hatlestad-Hall, C., Rygvol, T. W. & Andersson, S. Bids-structured resting-state electroencephalography (eeg) data extracted from an experimental paradigm. *Data Brief* **45**, 108647 (2022).

88. Liu, H. *et al.* An eeg motor imagery dataset for brain computer interface in acute stroke patients. *Sci. Data* **11**, 131 (2024).

89. Rockhill, A. P., Jackson, N., George, J., Aron, A. & Swann, N. C. "uc san diego resting state eeg data from patients with parkinson's disease", DOI: [doi:10.18112/openneuro.ds002778.v1.0.5](https://doi.org/10.18112/openneuro.ds002778.v1.0.5) (2021).
90. Anjum, M. F. *et al.* Linear predictive coding distinguishes spectral eeg features of parkinson's disease. *Park. & related disorders* **79**, 79–85 (2020).
91. Cavanagh, J. F., Kumar, P., Mueller, A. A., Richardson, S. P. & Mueen, A. Diminished eeg habituation to novel events effectively classifies parkinson's patients. *Clin. Neurophysiol.* **129**, 409–418 (2018).
92. Vicchietti, M. L., Ramos, F. M., Betting, L. E. & Campanharo, A. S. Computational methods of eeg signals analysis for alzheimer's disease classification. *Sci. Reports* **13**, 8184 (2023).
93. Stevenson, N. J., Tapani, K., Lauronen, L. & Vanhatalo, S. A dataset of neonatal eeg recordings with seizure annotations. *Sci. data* **6**, 1–8 (2019).
94. Ge, W. *et al.* Deep active learning for interictal ictal injury continuum eeg patterns. *J. neuroscience methods* **351**, 108966 (2021).
95. Xiang, C., Fan, X., Bai, D., Lv, K. & Lei, X. A resting-state eeg dataset for sleep deprivation. *Sci. Data* **11**, 427 (2024).
96. Trinh, N., Whelan, R., Ward, T. & Derosiere, G. Task-related and resting-state eeg classification of adult patients with adhd using machine learning. In *2023 IEEE 19th International Conference on Body Sensor Networks (BSN)*, 1–4 (IEEE, 2023).
97. Motie Nasrabadi, A., Allahverdy, A., Samavati, M. & Mohammadi, M. R. Eeg data for adhd/control children. *(No Title)* (2020).
98. Olejarczyk, E. & Jernajczyk, W. Graph-based analysis of brain connectivity in schizophrenia. *PloS one* **12**, e0188629 (2017).
99. jcavanagh@unm.edu, J. F. C. "eeg: Depression rest", DOI: [10.18112/openneuro.ds003478.v1.1.0](https://doi.org/10.18112/openneuro.ds003478.v1.1.0) (2021).
100. Mumtaz, W. Mdd patients and healthy controls eeg data (new). *figshare, Dataset* (2016).
101. Miltiadous, A. *et al.* A dataset of scalp eeg recordings of alzheimer's disease, frontotemporal dementia and healthy subjects from routine eeg. *Data* **8**, 95 (2023).
102. Blankertz, B., Dornhege, G., Krauledat, M., Müller, K.-R. & Curio, G. The non-invasive berlin brain–computer interface: fast acquisition of effective performance in untrained subjects. *NeuroImage* **37**, 539–550 (2007).
103. Savran, A. *et al.* Emotion detection in the loop from brain signals and facial images. In *Summer Workshop on Multimodal Interfaces (eINTERFACE 2006)*, 69–80 (2006).
104. Luciw, M. D., Jarocka, E. & Edin, B. B. Multi-channel eeg recordings during 3,936 grasp and lift trials with varying weight and friction. *Sci. data* **1**, 1–11 (2014).
105. Margaux, P., Emmanuel, M., Sébastien, D., Olivier, B. & Jérémie, M. Objective and subjective evaluation of online error correction during p300-based spelling. *Adv. Human-Computer Interact.* **2012**, 578295 (2012).
106. Schalk, G., McFarland, D. J., Hinterberger, T., Birbaumer, N. & Wolpaw, J. R. Bci2000: a general-purpose brain-computer interface (bci) system. *IEEE Transactions on biomedical engineering* **51**, 1034–1043 (2004).
107. Trujillo, L. T. Mental effort and information-processing costs are inversely related to global brain free energy during visual categorization. *Front. neuroscience* **13**, 1292 (2019).
108. Trujillo, L. T., Stanfield, C. T. & Vela, R. D. The effect of electroencephalogram (eeg) reference choice on information-theoretic measures of the complexity and integration of eeg signals. *Front. neuroscience* **11**, 425 (2017).
109. Zheng, W.-L. & Lu, B.-L. Investigating critical frequency bands and channels for eeg-based emotion recognition with deep neural networks. *IEEE Transactions on autonomous mental development* **7**, 162–175 (2015).

110. Zheng, W.-L., Liu, W., Lu, Y., Lu, B.-L. & Cichocki, A. Emotionmeter: A multimodal framework for recognizing human emotions. *IEEE transactions on cybernetics* **49**, 1110–1122 (2018).

111. Liu, W. *et al.* Identifying similarities and differences in emotion recognition with eeg and eye movements among chinese, german, and french people. *J. Neural Eng.* **19**, 026012 (2022).

112. Torkamani-Azar, M., Kanik, S. D., Aydin, S. & Cetin, M. Prediction of reaction time and vigilance variability from spatio-spectral features of resting-state eeg in a long sustained attention task. *IEEE journal biomedical health informatics* **24**, 2550–2558 (2020).

113. Korczowski, L. *et al.* *Brain Invaders calibration-less P300-based BCI with modulation of flash duration Dataset (bi2015a)*. Ph.D. thesis, GIPSA-lab (2019).

114. Jiang, W.-B., Zhao, L.-M., Guo, P. & Lu, B.-L. Discriminating surprise and anger from eeg and eye movements with a graph network. In *2021 IEEE International Conference on Bioinformatics and Biomedicine (BIBM)*, 1353–1357 (IEEE, 2021).

115. Jiang, W.-B., Liu, X.-H., Zheng, W.-L. & Lu, B.-L. Multimodal adaptive emotion transformer with flexible modality inputs on a novel dataset with continuous labels. In *proceedings of the 31st ACM international conference on multimedia*, 5975–5984 (2023).

116. Luo, S. *et al.* Multimodal emotion recognition in response to oil paintings. In *2022 44th Annual International Conference of the IEEE Engineering in Medicine & Biology Society (EMBC)*, 4167–4170 (IEEE, 2022).

117. Li, R., Liu, L.-D. & Lu, B.-L. Discrimination of decision confidence levels from eeg signals. In *2021 10th International IEEE/EMBS Conference on Neural Engineering (NER)*, 946–949 (IEEE, 2021).

118. Tao, L.-Y. & Lu, B.-L. Emotion recognition under sleep deprivation using a multimodal residual lstm network. In *2020 International Joint Conference on Neural Networks (IJCNN)*, 1–8 (IEEE, 2020).

119. He, Y., Luu, T. P., Nathan, K., Nakagome, S. & Contreras-Vidal, J. L. A mobile brain-body imaging dataset recorded during treadmill walking with a brain-computer interface. *Sci. data* **5**, 1–10 (2018).

120. Brunner, C., Leeb, R., Müller-Putz, G., Schlögl, A. & Pfurtscheller, G. Bci competition 2008–graz data set a. *Inst. for knowledge discovery (laboratory brain-computer interfaces)*, *Graz Univ. Technol.* **16**, 34 (2008).

121. Zyma, I. *et al.* Electroencephalograms during mental arithmetic task performance. *Data* **4**, 14 (2019).

122. Nejedly, P. *et al.* Multicenter intracranial eeg dataset for classification of graphoelements and artifactual signals. *Sci. data* **7**, 179 (2020).

123. Van Den Oord, A., Vinyals, O. *et al.* Neural discrete representation learning. *Adv. neural information processing systems* **30** (2017).

124. He, K. *et al.* Masked autoencoders are scalable vision learners. In *Proceedings of the IEEE/CVF conference on computer vision and pattern recognition*, 16000–16009 (2022).

125. Kostas, D., Aroca-Ouellette, S. & Rudzicz, F. Bendl: Using transformers and a contrastive self-supervised learning task to learn from massive amounts of eeg data. *Front. Hum. Neurosci.* **15**, 653659 (2021).

126. Oikonomou, V. P., Georgiadis, K., Liaros, G., Nikolopoulos, S. & Kompatsiaris, I. A comparison study on eeg signal processing techniques using motor imagery eeg data. In *2017 IEEE 30th international symposium on computer-based medical systems (CBMS)*, 781–786 (IEEE, 2017).

127. Schirrmeister, R. T. *et al.* Deep learning with convolutional neural networks for eeg decoding and visualization. *Hum. brain mapping* **38**, 5391–5420 (2017).

128. Amin, S. U., Alsulaiman, M., Muhammad, G., Mekhtiche, M. A. & Hossain, M. S. Deep learning for eeg motor imagery classification based on multi-layer cnns feature fusion. *Futur. Gener. computer systems* **101**, 542–554 (2019).

129. Zhang, D., Chen, K., Jian, D. & Yao, L. Motor imagery classification via temporal attention cues of graph embedded eeg signals. *IEEE journal biomedical health informatics* **24**, 2570–2579 (2020).

130. Potter, I. Y., Zerveas, G., Eickhoff, C. & Duncan, D. Unsupervised multivariate time-series transformers for seizure identification on eeg. In *2022 21st IEEE International Conference on Machine Learning and Applications (ICMLA)*, 1304–1311 (IEEE, 2022).

131. Woo, G., Liu, C., Sahoo, D., Kumar, A. & Hoi, S. Cost: Contrastive learning of disentangled seasonal-trend representations for time series forecasting. *arXiv preprint arXiv:2202.01575* (2022).

132. Zhang, X., Zhao, Z., Tsiligkaridis, T. & Zitnik, M. Self-supervised contrastive pre-training for time series via time-frequency consistency. *Adv. neural information processing systems* **35**, 3988–4003 (2022).

133. Nie, Y., Nguyen, N. H., Sinthong, P. & Kalagnanam, J. A Time Series is Worth 64 Words: Long-term Forecasting with Transformers, DOI: [10.48550/arXiv.2211.14730](https://doi.org/10.48550/arXiv.2211.14730) (2023). [2211.14730](https://doi.org/10.48550/arXiv.2211.14730).

134. Eldele, E. *et al.* Time-series representation learning via temporal and contextual contrasting. *arXiv preprint arXiv:2106.14112* (2021).

135. Zhang, Z. & Parhi, K. K. Low-complexity seizure prediction from ieeg/seeg using spectral power and ratios of spectral power. *IEEE transactions on biomedical circuits systems* **10**, 693–706 (2015).

136. Handa, P. & Goel, N. Epileptic seizure detection using rhythmicity spectrogram and cross-patient test set. In *2021 8th international conference on signal processing and integrated networks (SPIN)*, 898–902 (IEEE, 2021).

137. Kadivar, M., Moghadam, E. M., Shervin Badv, R., Sangsari, R. & Saeedy, M. A comparison of conventional electroencephalography with amplitude-integrated eeg in detection of neonatal seizures. *Med. Devices: Evid. Res.* 489–496 (2019).

138. Wang, Y. *et al.* Seeg-net: An explainable and deep learning-based cross-subject pathological activity detection method for drug-resistant epilepsy. *Comput. Biol. Medicine* **148**, 105703 (2022).

139. Jing, J. *et al.* Development of expert-level classification of seizures and rhythmic and periodic patterns during eeg interpretation. *Neurology* **100**, e1750–e1762 (2023).

140. Yang, C., Xiao, D., Westover, M. B. & Sun, J. Self-supervised eeg representation learning for automatic sleep staging. *arXiv preprint arXiv:2110.15278* (2021).

141. Peh, W. Y., Yao, Y. & Dauwels, J. Transformer convolutional neural networks for automated artifact detection in scalp eeg. In *2022 44th Annual International Conference of the IEEE Engineering in Medicine & Biology Society (EMBC)*, 3599–3602 (IEEE, 2022).

142. Li, H., Ding, M., Zhang, R. & Xiu, C. Motor imagery eeg classification algorithm based on cnn-lstm feature fusion network. *Biomed. signal processing control* **72**, 103342 (2022).

143. Song, Y., Jia, X., Yang, L. & Xie, L. Transformer-based spatial-temporal feature learning for eeg decoding. *arXiv preprint arXiv:2106.11170* (2021).

144. Bai, S., Kolter, J. Z. & Koltun, V. An empirical evaluation of generic convolutional and recurrent networks for sequence modeling. *arXiv preprint arXiv:1803.01271* (2018).

145. Tang, S. *et al.* Self-supervised graph neural networks for improved electroencephalographic seizure analysis. *arXiv preprint arXiv:2104.08336* (2021).

146. Tang, S. *et al.* Modeling multivariate biosignals with graph neural networks and structured state space models. In *Conference on health, inference, and learning*, 50–71 (PMLR, 2023).

147. Hochreiter, S. & Schmidhuber, J. Long short-term memory. *Neural computation* **9**, 1735–1780 (1997).

148. Liu, Z. *et al.* A convnet for the 2020s. In *Proceedings of the IEEE/CVF conference on computer vision and pattern recognition*, 11976–11986 (2022).

149. Goswami, M. *et al.* Moment: A family of open time-series foundation models. *arXiv preprint arXiv:2402.03885* (2024).

150. Wu, H. *et al.* Timesnet: Temporal 2d-variation modeling for general time series analysis. *arXiv preprint arXiv:2210.02186* (2022).

151. Nie, Y., Nguyen, N. H., Sinthong, P. & Kalagnanam, J. A time series is worth 64 words: Long-term forecasting with transformers. *arXiv preprint arXiv:2211.14730* (2022).

152. Mivalt, F. *et al.* Impedance rhythms in human limbic system. *J. Neurosci.* **43**, 6653–6666 (2023).

153. Kiessner, A.-K., Schirrmeister, R. T., Boedecker, J. & Ball, T. Reaching the ceiling? empirical scaling behaviour for deep eeg pathology classification. *Comput. Biol. Medicine* **178**, 108681 (2024).

154. Klonowski, W. Everything you wanted to ask about eeg but were afraid to get the right answer. *Nonlinear biomedical physics* **3**, 1–5 (2009).

155. Donoghue, T. *et al.* Parameterizing neural power spectra into periodic and aperiodic components. *Nat. neuroscience* **23**, 1655–1665 (2020).

156. Peng, Z., Dong, L., Bao, H., Ye, Q. & Wei, F. Beit v2: Masked image modeling with vector-quantized visual tokenizers. *arXiv preprint arXiv:2208.06366* (2022).

157. Wang, Y. *et al.* Deep time series models: A comprehensive survey and benchmark. *arXiv preprint arXiv:2407.13278* (2024).

158. Wan, Z., Yu, Q., Mao, J., Duan, W. & Ding, C. Openecg: Benchmarking ecg foundation models with public 1.2 million records. *arXiv preprint arXiv:2503.00711* (2025).

159. Arora, S. *et al.* On the evaluation of speech foundation models for spoken language understanding. *arXiv preprint arXiv:2406.10083* (2024).

160. Wei, X. *et al.* 2021 beetl competition: Advancing transfer learning for subject independence and heterogenous eeg data sets. In *NeurIPS 2021 Competitions and Demonstrations Track*, 205–219 (PMLR, 2022).

161. Jing, J. *et al.* Hms - harmful brain activity classification. <https://kaggle.com/competitions/hms-harmful-brain-activity-classification> (2024). Kaggle.

162. Reyna, M. A. *et al.* Predicting neurological recovery from coma after cardiac arrest: The george b. moody physionet challenge 2023. In *2023 Computing in Cardiology (CinC)*, vol. 50, 1–4 (IEEE, 2023).

163. Dan, J. *et al.* Szcore: Seizure community open-source research evaluation framework for the validation of electroencephalography-based automated seizure detection algorithms. *Epilepsia* (2024).

164. Gramfort, A. *et al.* Meg and eeg data analysis with mne-python. *Front. Neuroinformatics* **7**, 267 (2013).

165. Schirrmeister, R. T. *et al.* Deep learning with convolutional neural networks for eeg decoding and visualization. *Hum. Brain Mapp.* DOI: [10.1002/hbm.23730](https://doi.org/10.1002/hbm.23730) (2017).

166. Schiratti, J.-B., Le Douget, J.-E., Le Van Quyen, M., Essid, S. & Gramfort, A. An ensemble learning approach to detect epileptic seizures from long intracranial eeg recordings. In *2018 IEEE International Conference on Acoustics, Speech and Signal Processing (ICASSP)*, 856–860 (IEEE, 2018).

167. McMahan, B., Moore, E., Ramage, D., Hampson, S. & y Arcas, B. A. Communication-efficient learning of deep networks from decentralized data. In *Artificial intelligence and statistics*, 1273–1282 (PMLR, 2017).

168. Tatum IV, W. O. *et al.* American clinical neurophysiology society guideline 7: guidelines for eeg reporting. *The Neurodiagnostic J.* **56**, 285–293 (2016).

169. Hinton, G., Vinyals, O. & Dean, J. Distilling the knowledge in a neural network. *arXiv preprint arXiv:1503.02531* (2015).

170. Han, S., Mao, H. & Dally, W. J. Deep compression: Compressing deep neural networks with pruning, trained quantization and huffman coding. *arXiv preprint arXiv:1510.00149* (2015).

171. Gong, Y., Liu, L., Yang, M. & Bourdev, L. Compressing deep convolutional networks using vector quantization. *arXiv preprint arXiv:1412.6115* (2014).
172. Mitchell, M. *et al.* Model cards for model reporting. In *Proceedings of the conference on fairness, accountability, and transparency*, 220–229 (2019).

Supplement

Table 3. *Channel-hours* were used to represent and compare the data scale at which the EEG-FMs were pretrained. In most cases, channel-hours per dataset were calculated as the product of the number of channels and the recording durations (in hours) obtained from the original studies. Scalp EEG datasets had a fixed channel count across subjects, whereas iEEG datasets, used by BrainBERT and Brant, had a subject-specific count. For Neuro-GPT and EEGFormer, channel-hours were computed from publicly available dataset statistics and were assumed to be applicable to both studies. For BrainWave, the total patch count reported was used to calculate the channel-hours by converting the patch size (1 second) to hours. Channel-hours pooled across all pretraining data sources are highlighted in bold. N/A represents cases where channel-hours could not be determined.

EEG-FM	Pretraining Dataset	Number of Channels	Total Length of Recordings (Hours)	Channel-Hours (= Number of Channels × Recording Length)	Total Channel-Hours
BrainBERT	Brain TreeBank ⁸⁰	-	-	$91 \times (1.83 + 1.75 + 0.5) + 100 \times (2.42 + 2.42 + 2.5 + 3 + 4.33 + 1.75 + 3.42) + 91 \times (1.92 + 2.67 + 93.92) + 135 \times (2.58 + 1.33 + 1.83) + 205 \times (1.75 + 1.77) + 152 \times (1.15 + 1.68 + 2.43) + (109 \times 1.5) + (102 \times 2.28) + (72 \times 1.28) + 173 \times (1.58 + 2.17)$	14,752.68
Neuro-GPT	TUEG ⁸³	20	27,063	541,260	541,260
Brant	Private dataset (unknown source)	-	-	$(124 \times 235.34) + (52 \times 82.39) + (120 \times 393.09) + (133 \times 137.45) + (116 \times 214.22) + (101 \times 386.70) + (67 \times 111.55) + (47 \times 207.42) + (134 \times 759.80)$	281,860.10
BIOT	SHHS ^{76,85}	2	42,446	84,892	
	PREST	16	14,197	227,152	312,044
EEGFormer	TUEG	20	27,063	541,260	541,260
LaBraM	BCI Competition IV-1 ¹⁰²	59	8.21	484.39	
	Emobrain ¹⁰³	64	4.94	316.16	
	Grasp/Lift EEG Challenge ¹⁰⁴	32	11.72	375.04	
	Inria BCI Challenge ¹⁰⁵	56	29.98	1,678.88	
	EEG Motor Imagery Dataset ¹⁰⁶	64	47.3	3,027.2	
	Visual Categorization EEG Data ¹⁰⁷	64	34.35	2,198.4	
	Resting State EEG Data ¹⁰⁸	64	3.04	194.56	
	SEED Series ¹⁰⁹⁻¹¹¹	62	166.75	10,338.5	
	Siena Scalp EEG Database ⁸⁴	31	30.47	944.57	
	SPIS Resting State Dataset ¹¹²	64	0.83	53.12	
	Brain-Invaders ¹¹³	32	16	512	
	TUAR ⁸³	23	92.22	2,121.06	
	TUEP ⁸³	21	591.22	12,415.62	
	TUSZ ⁸³	21	1,138.53	23,909.13	
	TUSI ⁸³	23	20.59	473.57	
	Multiple data sources ¹¹⁴⁻¹¹⁸	62	342.23	21,218.26	80,260.46
Mentality	TUSZ	N/A	N/A	N/A	N/A
NeuroLM	TUEG	21	24,000	504,000	
	SEED Series	62	170.54	10,573.48	
	BCI Competition IV-1	59	8.21	484.39	
	Emobrain	64	4.94	316.16	
	Grasp/Lift EEG Challenge	32	11.72	375.04	
	Inria BCI Challenge	56	29.98	1,678.88	
	Motor Movement/Imagery Dataset	64	47.3	3,027.2	
	Raw EEG Data	64	34.35	2,198.4	
	Resting State EEG Data	64	3.04	194.56	
	Siena Scalp EEG Database	31	30.47	944.57	
	SPIS Resting State Dataset	64	0.83	53.12	
	Brain-Invaders	32	16	512	
	Multiple data sources ¹¹⁴⁻¹¹⁸	62	342.23	21,218.26	545,576.06
FoME	Multiple datasets	N/A	N/A	N/A	N/A
BrainWave	Multiple datasets	-	-	$3,162,233,694 \times (1 \div 3,600)$	878,398.25